Study on cucumber mosaic virus resistance conferred by an in-frame deletion in genome-edited tomato *eIF4E1*

トマト *eIF4E1* のゲノム編集によるインフレーム欠失変異により付与されるキュウリモザイクウイルス抵抗性に関する研究

Graduate School of Agriculture, Hokkaido University

Division of Agriculture, Frontiers in Production Sciences

Doctoral Course

SOZIB GHOS

TABLE OF CONTENTS

LIST OF FIGURES

LIST OF TABLES

ABBREVIATIONS

eIF4E	Eukaryotic Translation Initiation Factor 4E
9DEL-eIF4E1	9-nucleotide deletion mutant of eIF4E1
RSS	RNA Silencing Suppressor
CMV	Cucumber mosaic virus
CMVΔ2b	CMV mutant lacking 2b protein
CMV2bΔC	CMV 2b mutant with C-terminal deletion
CRISPR	Clustered Regularly Interspaced Short Palindromic Repeats
DCL	Dicer-like
siRNA	Small Interfering RNA
VSR	Viral Suppressor of RNA Silencing
NB	Nicotiana benthamiana
WT	Wild Type
Y2H	Yeast Two-Hybrid
CBB	Coomassie Brilliant Blue
BTH	Benzothiadiazole
D.W.	Distilled water
SA	Salicylic acid
JA	Jasmonic acid

GENERAL INTRODUCTION

Viruses are among the most challenging pathogens affecting global agriculture, causing extensive crop damage, reducing food security, and significant economic losses. Intensified crop monoculture, vector proliferation, and climate change all contribute to the global impact of viral diseases. Because of the limited effectiveness of traditional control measures against plant viruses, such as the use of pesticides and cultural practices, the development of genetically resistant cultivars is required as a durable and sustainable solution.

Cucumber mosaic virus (CMV) is a widely distributed and agriculturally destructive virus. CMV has a broad host range, infecting over 1200 plant species, including vegetables, fruits, and ornamental plants. It ranks as the fourth most significant among all plant viruses (**Zitter and Murphy, 2009; Scholthof et al., 2011**). CMV is particularly devastating in tomato (*Solanum lycopersicum*), where it induces symptoms such as mosaic pattern, chlorosis, leaf distortion, stunted growth, fruit malformation, and death in severe case, ultimately leading to substantial economic losses (**Pagán, 2019; Hirsch and Moury, 2021**). CMV is predominantly transmitted by aphids in a non-persistent manner and occasionally through seeds, which enables widespread dissemination across regions and cropping systems (**Tatineni and Hein, 2023**).

CMV is a positive-sense single-stranded RNA virus belonging to the genus *Cucumovirus* within the family *Bromoviridae*. The CMV genome comprises three segments, RNA1, RNA2, and RNA3, along with two sub-genomic RNAs (RNA4 and RNA4A), which together encode five major proteins: 1a, 2a, 3a (movement protein), and 3b (coat protein)

translated from RNA1, RNA2, RNA3, and sub-genomic RNA4, respectively. While the 2b, an RNA silencing suppressor protein is encoded by RNA2 but is translated from the sub-genomic RNA4A at the 3′ ends of RNA2 (**Palukaitis, 2019**). Among these CMV proteins, the 2b protein plays a pivotal role in overcoming plant defenses. 2b is a multifunctional virulence determinant that enhances pathogenicity by suppressing post-transcriptional gene silencing (PTGS), altering hormone (SA and JA) signaling, affects host gene expression, increases viral accumulation, and facilitating systemic viral movement (**Lewsey et al., 2009; Zhang et al., 2024; Crawshaw et al., 2024**).

The virulence and functionality of 2b vary across the CMV strains. Strain-specific amino acid sequence variants of 2b such as R2b, Y2b, and HL2b differ in their RNA silencing suppressor (RSS) activity and pathogenicity, attributed to specific amino acid substitutions, particularly in the C-terminal region revealed in sequence alignment, which is essential for nuclear localization and host protein interaction (**Goto et al., 2007; Sueda et al., 2010**). For example, A2b from CM95 strain and R2b from CM95R strain differ by a single amino acid at the position 46 (C to R). While Y2b from CMV-Y strain shares a significant sequence similarity (>90%) with R2b but contains unique substitutions, both belongs to the subgroup I, and the HL2b from lily-CMV strain in the subgroup IA, shows ~80–85% sequence similarity, induces necrotic spots on infected *Arabidopsis* but fails to interact with certain host proteins due to unique C-terminal residues, unlike subgroup I strain like CMV-Y (**Goto et al., 2007; Sueda et al., 2010; Masuta et al., 2012; Kim et al., 2022**). In contrast, 2b from CMV (Ho) mutant belongs to subgroup IA, sharing over 85% amino acid sequence similarity with other virulent subgroup IA isolates like HL2b, is asymptomatic in *Arabidopsis thaliana*, indicating that even a single or limited number of substitutions in 2b

can cause substantial differences in symptoms (**Takahashi et al., 2022**). These sequence changes may modulate its interaction with host factors, affecting CMV pathogenicity and symptom development.

The functional significance of the 2b varies on the host plant species, highlighting differences in host plant-virus interactions. The 2b protein has multifunctional role in virulence. In *Arabidopsis thaliana,* 2b from CMV-Fny strain, a well-characterized subgroup IA isolate, acts as a potent RNA silencing suppressor, a key antiviral response by binding small RNAs and interfering with Argonaute1 (AGO1)-mediated cleavage (**Zhao et al., 2018**). It also binds to double-stranded small RNAs and AGO proteins, impairing the RNA-induced silencing complex (RISC) and facilitating systemic infection (**Zhang et al., 2006; González et al., 2010**). Previous studies have demonstrated that interference with 2b's activity or localization impairs CMV virulence (**Du et al., 2014**). Besides its RNA silencing suppression activity (RSS), 2b interacts with several host proteins. Fny2b binds to catalase (CAT3) in *Arabidopsis*, affecting its hydrogen peroxide breakdown function, leading to necrosis and enhanced viral accumulation (**Murota et al., 2017**). Similarly, Fny2b interacts with ribosomal subunit protein S11 (RPS11) to promote CMV replication and RSS activity, which is essential for systemic CMV infection in *Nicotiana benthamiana* (**Wang et al., 2017**). 2b from CMV-LS, a subgroup I isolate, suppresses the host RNA silencing, facilitates viral RNA accumulation, and enables systemic infection in *Nicotiana clevelandii* and *Nicotiana glutinosa* (**Shi and Palukaitis, 2011**). However, the requirement of 2b for CMV systemic infection is host-dependent. In *Nicotiana tabacum*, Fny2b enhance systemic infection and symptom severity by suppressing RNA silencing and facilitating viral movement to the shoot apical meristem and leaf primordia, but CMVΔ2b (lacking 2b)

able to achieve systemic infection highlights that 2b is not essential for systemic infection in tobacco (**Sunpapao et al., 2009**).

In addition, 2b has been also identified as a pivotal factor in suppressing host defenses by modulating host defense-related hormonal pathways, such as those mediated by salicylic acid (SA) and jasmonic acid (JA). 2b disrupts RNA silencing and modulates both salicylic acid (SA) and jasmonic acid (JA) signaling pathways, promoting systemic infection and symptom severity of CMV in tomato (**Lewsey et al., 2009; Khaing et al., 2020a**). In *Nicotiana benthamiana*, 2b interacts with HSP90s, preventing SA-induced degradation of NPR3, stabilizing NPR3 (a negative regulator of SA signaling), inhibiting NPR1 activation (a positive key regulator), reducing *PR1* gene expression, and facilitating CMV infection (**Zhang et al., 2024**). In *Arabidopsis thaliana*, 2b binds to AGO1, inhibiting RNA silencing, downregulating NPR1, and suppressing SA-mediated defense signaling (**Shukla et al., 2022; Crawshaw et al., 2024**). Further, 2b binds to AGO1, interfering with JA signaling downstream of the CORONATINE-INSENSITIVE1 (*COI1*) receptor, suppressing JA-responsive genes, such as *PDF1.2* and *VSP2*, and weakening plant defenses against herbivores and pathogens (**Arinaitwe et al., 2023; Crawshaw et al., 2024**). 2b also interacts with jasmonate ZIM-domain (JAZ) proteins, preventing *COI1*-mediated degradation of JAZ, which reduces JA-related insect repellence, enhances aphid attraction, and facilitating virus transmission (**Ziebell et al., 2011; Wu et al., 2017**). It also disrupts JA biosynthesis by targeting allene oxide cyclase (AOC) through interaction with cpSRP54, reducing JA synthesis and further compromising JA-mediated defense (**Ji et al., 2021**). The C-terminal of 2b is critical for suppressing salicylic acid (SA)- mediated

defenses and ensuring efficient CMV systemic infection and transmission (**Ziebell et al., 2011; Zhou et al., 2014**).

Given the central role of 2b in CMV pathogenicity, it is a promising target for virus resistance. However, the successful infection and systemic movement of CMV, like many plant viruses, relies not only on viral proteins but also on specific host factors that facilitate viral RNA replication and protein translation. One of the most prominent susceptibility factors is eukaryotic translation initiation factor 4E (eIF4E), which facilitates cap-dependent translation in eukaryotes for viral proliferation. The eIF4E protein binds the 5´-cap structure of mRNA and recruits it to the ribosome for translation initiation, a process hijacked by many viral proteins such as VPg or RSS proteins for viral replication (**Zlobin and Taranov, 2023; Zhou et al., 2024**). Tomato has two eIF4E isoforms, eIF4E1 and eIF4E2. Several studies have revealed that potyviruses, cucumoviruses, and other +ssRNA viruses directly interact with eIF4E or its isoforms to facilitate infection (**Gauffier et al., 2016; Piron et al., 2010**). Mutations in eIF4E disrupt these interactions, conferring the host resistance to the viruses without significantly impairing plant viability. Natural and induced mutations in the eIF4E gene have been shown to confer recessive resistance to a variety of RNA viruses in different crops (**Nicaise et al., 2003; Ruffel et al., 2002**). This form of resistance is often durable and broad-spectrum, making eIF4E an attractive target for crop improvement. Natural eIF4E mutations, such as *D55G* in tobacco, confer resistance to potato virus Y (PVY), while *D71G* in watermelon disrupts the VPg–eIF4E interaction, conferring resistance to papaya ringspot virus-watermelon strain (PRSV-W), zucchini yellow mosaic virus (ZYMV), and watermelon mosaic virus (WMV) (**Zhou et al., 2024**). Similarly, the natural mutation *Ala64Val* in sugarcane eIF4E prevents interaction with the

VPg, impairing viral replication and conferring resistance to sugarcane streak mosaic virus (SCSMV) (**Shan et al., 2023**).

The advancement of precise genome editing technologies, particularly CRISPR/Cas9 or TILLING, has enabled targeted mutations in susceptibility genes like *eIF4E1* for developing novel virus-resistant crops to multiple potyviruses. While complete gene knockouts have proven to confer broad-spectrum resistance, they can also cause growth defects because of the essential role of eIF4E in translation initiation (**Mazier et al., 2011; Gauffier et al., 2016**). Many potyviruses, such as pepper mottle virus (PepMoV), clover yellow vein virus (ClYVV), and pepper veinal mottle virus (PVMV), conferred resistance by eIF4E CRISPR/Cas9 editing (**Bastet et al., 2019; Moury et al., 2020; Yoon et al., 2020; Kuroiwa et al., 2022**). Although gene redundancy may affect resistance, TILLING-induced mutations inhibited the expression of eIF4E, preventing it from interacting with a viral protein and conferring resistance to PVY and PepMoV (**Piron et al., 2010; Gauffier et al., 2016**). Broad-spectrum resistance to potyviruses such as PVY, PepMoV, tobacco etch virus (TEV), soybean mosaic virus (SMV), bean common mosaic virus (BCMV), and watermelon mosaic virus (WMV) was achieved by RNAi-mediated silencing of eIF4E1 and eIF4E2, although the plant growth was impaired, but it reduced the viral interaction and virus accumulation (**Mazier et al., 2011; Gao et al., 2020**). To address these limitations, in-frame deletions or point mutations offer an alternative approach by maintaining partial functionality while disrupting virus-specific interactions (**Bastet et al., 2019; Nekrasov et al., 2017**).

In a previous study by **Atarashi et al. (2020),** a tomato (*Solanum lycopersicum* L.) cultivar ‘S8’ was CRISPR/Cas9-edited in the second half of the eIF4E1 coding region to generate

three different alleles of *eIF4E1*: A knockout allele with a 1-nucleotide insertion (*1INS*), a 3-nucleotide deletion (*3DEL*), and a 9-nucleotide in-frame deletion (*9DEL*). The *1INS* line was resistant to PVY but remained susceptible to CMV. It was unable to produce functional protein, because of a frameshift caused by the 1-nucleotide deletion in the first exon. In comparison, *9DEL* conferred partial resistance to CMV while remaining susceptible to PVY, making it a unique *eIF4E1* resistance allele. Inoculation of *1INS* tomato suggested that eIF4E1 is needed for PVY, but not for CMV infection. Since eIF4E1 retains its function for tested PVY infection, we hypothesized that the mutated eIF4E1 (9DEL-eIF4E1) protein from *9DEL* tomato has acquired an inhibitory function against CMV infection.

The objective of this study was to investigate the interaction between 9DEL-eIF4E1 and CMV viral proteins, and to elucidate the molecular basis of this unique partial CMV resistance mechanism conferred by *9DEL*. The findings propose a novel resistance strategy based on targeted in-frame genome editing.

MATERIALS AND METHODS

1. Plant and virus materials

Wild-type tomato (*Solanum lycopersicum* L.) cultivar 'S8', cultivar 'Moneymaker', previously CRISPR/Cas edited *9DEL* tomato (**Atarashi et al. 2020**), *Nicotiana benthamiana* and *ATG7ko N. benthamiana* (lacking autophagy, *ATG7* knockout mutant of *Nicotiana benthamiana,* provided by Dr. Kenji Nakahara, details regarding its generation and other characteristics are currently restricted from disclosure) plants were grown in a plant growth chamber at 25°C under a 16-hour light and 8-hour dark cycle.

The CMV-Y (**Kataoka et al. 1990**), and its site-directed mutant variants (**Ryabov et al. 2001; Tungadi et al. 2017**), 2b protein lacking CMVΔ2b (**Matsuo et al. 2007**), and its C-terminal truncated CMV-2bΔC (**Otagaki et al. 2006**), were stored in a deep freezer at -80°C, used as inoculum for the inoculation tests in this study. CMV-Y, CMV-R95, and lily-derived CMV-HL strain were the source of Y2b, R2b, and HL2b protein (**Kataoka et al. 1990; Goto et al. 2007; Masuta et al. 2012**).

2. Plasmids for Yeast Two-Hybrid

Previously constructed plasmids were used for the yeast two-hybrid (Y2H) assay. pGADT7 was used as the prey vector and pGBT9 was used for the bait vector from the Matchmaker^{TM} GAL4 Two-Hybrid System 3 (Clontech Laboratories, Mountain View, CA, USA). After *DpnI* restriction digestion, the insert was purified by a MonoFas® DNA purification Kit 1 following manufacturers manual and then cloned by ligation reaction (**Table 1**) at 16°C for 30 min.

Table 1: Ligation mixture.

Reagents	Volume (10 µl)
Vector	1 µl
Insert	2 µl
2x rapid ligation buffer (Promega, Madison, WI, USA)	5 µl
T4 ligase (Promega, Madison, WI, USA)	1 µl
DW	1 µl

To introduce mutations in cloned target sequences in pGADT7 or pGBT9 vectors, inverse PCR was performed using the KOD OneTM PCR Master Mix Blue (Toyobo, Japan). The PCR reaction solution and the PCR condition are shown in **Table 2 and 3.** All the primers are listed in **Table 4.**

Table 2: Inverse PCR reaction solution.

Reagents	Volume (50 µl)
KOD OneTM PCR Master Mix Blue	25 µl
Forward primer (10 µM)	0.75 µl
Reverse primer (10 µM)	0.75 µl
Template plasmid DNA	1~50 ng/50 µl
DW	Up to 50 µl

Table 3: Inverse PCR conditions.

Starting	Denaturation	Annealing	Extension			Hold
94°C	98°C	60°C	68° C	30 Cycle	72° C	4° C
2 min	10 sec	30 sec	6 min		3 min	∞

Table 4: Primers used in inverse PCR.

Primer name	Sequence	Mutant product	Vector
R2b_A_primer_F	ATGGAATTGAACGCGGGTGCGATGAC	R2b_V5A	pGBT9-
R2b_A_primer_R	ACGGATCCCCGGGAATTCCGGCGATACAGTC	R2b_V5A	pGBT9-
R2b_R_primer_F	TGGAGGCGAAGAGACAGAGACGAAGG	R2b_K23R	pGBT9-
R2b_R_primer_R	CCATACGAGCCAGTTGGAGT	R2b_K23R	pGBT9-
R2b_F_primer_F	TTCCTACCGTTCTTTCAAGTGGATGG	R2b_Y58E	pGBT9-
R2b_F_primer_R	GCGGAACAGTCTGAGATTCGAA	R2b_Y58E	pGBT9-
R2b_L_primer_F	GGAAGACCATGATCTTGACGATACCG	R2b_F94L	pGBT9-
R2b_L_primer_R	GCCGATAACTCTAAACGAGA	R2b_F94L	pGBT9-
R2b_K_primer_F	GTTCGCCGGTAACAAATGGGCGGAAGG	R2b_E104K	pGBT9-
R2b_K_primer_R	CAATCGGTATCGTCAAAATCATGG	R2b_E104K	pGBT9-
HL2b_K104E_primer_F	GGTTCGCCGGTAACGAATGGGCGGAAGGAGCTTTCTGACTGCAG CCAAGCT	HL2b_L94F_K104 E, HL2b_K104E	pGBT9-
Pst I – R2b	AGCTTGGCTGCAGTCAGAAAGTACC	HL2b_L94F_K104 E, HL2b_K104E	pGBT9-
R2b_CDEL_primer_F	CATTGTGAATTCATGGAATTGAACGTAGGTGC	R2b_CDEL	pGBT9-
R2b_CDEL_primer_F	CAAGCTGGATCCCTAGTCAAAATCATGGTCTTCCG	R2b_CDEL	pGBT9-

The PCR products were digested with *DpnI* and purified using a MonoFas® DNA purification Kit l. T4 DNA ligase (Promega, Madison, WI, USA) was used for ligation at 16℃ for 30 min, and the ligation mixture (**Table 1**) was transformed into *E. coli* DH5α cells using heat shock at 42℃ for 30 sec and chilling on ice for 2 min. Transformants were analyzed by colony PCR (GoTaq®, Promega) following manufacturer's instructions and sequenced.

3. Yeast Two-Hybrid (Y2H) assay

TheY2H assay was performed using the Matchmaker^{TM} GAL4 Two-Hybrid System 3 (Clontech Laboratories, Mountain View, CA, USA) following the manufacturer's instructions. *Saccharomyces cerevisiae* strain Y2HGold was cultured in 10 ml liquid YPAD medium at 30℃ overnight with shaking. Fresh 40 ml YPAD was added and incubated for 3-4 hours until the concentration reached OD_{600} = 0.6-1.0. The culture suspension was centrifuged at 3000 rpm for 5 min and the supernatant was discarded to harvest the yeast

cells. 25 ml of D.W. was added and centrifuged at 3000 rpm for 5 min. After discarding the supernatant, 900 µl D.W. was added and centrifuged at 3000 rpm for 5 min, discarded the supernatant. The yeast cells were resuspended in 1 ml of 100 mM lithium acetate (LiAc), and incubated at room temperature for 10 min.

Table 5: Transformation solution.

Reagents	**Volume (360 µl)**
50% PEG-3350	240 µl
1M LiAc	36 µl
10mg/ml SSS DNA	5 µl
DMSO	36 µl
DW	43 µl

A total of 360 µl of transformation solution (**Table 5**), 100 µl of yeast cell suspension and 1 µl of respective plasmid DNA were added, and the mixture was vortexed. It was incubated for 30 min at 30℃, followed by an additional incubation at 42℃ for 30 min. It was centrifuged at 3000 rpm for 5 min and the supernatant was discarded. The pellets were resuspended in 500 µl of D.W. and 250 µl was spread on selective SD media lacking Leu/Trp (SD-LT), Leu/Trp/His (SD-LTH), or Leu/Trp/His/Ade (SD-LTHA). Plates were incubated for 3-4 days at 30℃. Protein interactions were observed based on yeast growth on selective media.

4. Agrobacterium infiltration

Agrobacterium tumefaciens LBA4404 competent cells (Takara Bio Inc., Kusatsu, Shiga, Japan) were thawed on ice. They were mixed with 300–500 ng of binary vector DNA, incubated on ice for 15-30 min, chilled in liquid nitrogen for 20 sec, and incubated at 37°C

for 5 min. Pre-warmed SOC medium (900 µl) was added; the mixture was incubated at 28°C for 4 hour with gentle shaking and centrifuged at 5000 rpm for 3 min. The pellets were resuspended in the remaining medium. Bacterial suspension was spread onto LB plates with appropriate antibiotics (kanamycin, streptomycin, rifampicin, hygromycin) for selection. The plates were incubated at 28°C for 2-3 days. Selected colonies were cultured in 4 ml LB broth supplemented with appropriate antibiotics (25 µl of a 50 mg/ml stock solution of each) and incubated at 28°C with gentle shaking for 48-hour. The suspension was centrifuged at 4000 rpm for 10 min; the pellets were resuspended in infiltration buffer (10 mM $MgCl_2$, 10 mM MES, 24 µl of Acetosyringone) and incubated at room temperature. The abaxial surface (underside) of *N. benthamiana* leaves were inoculated using a needleless plastic syringe loaded with the suspension. Inoculated plants were maintained at 25°C at 16-hour light and 8-hour darkness.

5. Co-localization test

At 4 days post-infiltration, infiltrated leaf sections were observed under a confocal microscope (All-in-One Fluorescence Microscope BZ-X800, KEYENCE, Osaka, Japan) to assess the subcellular localization and signal overlap of GFP and dsRed fluorescence.

6. Split luciferase complementation assay

Previously constructed binary vectors express PVX CP and R2b were fused to N-terminal fragment of luciferase (nLuc), while C-terminal fragment (cLuc) was fused to R2b, eIF4E1, and 9DEL-eIF4E1, under the control of CaMV 35S promoter. The co-infiltrated combinations were R2b x PVX CP, 9DEL-eIF4E1 x R2b, 9DEL-eIF4E1 x PVX CP, R2b x R2b (as a positive control), eIF4E1 x R2b, and eIF4E1 x PVX CP, where PVX CP combinations served as a negative control. *N. benthamiana* leaves were agrobacterium-

infiltrated as described above, and the plants were maintained at 25°C at 16 hours light and 8 hours darkness for 35 to 38 hours. Infiltrated leaves were sprayed with 1 mM D-luciferin solution and incubated in the darkness for 7 min. The chemiluminescence luciferase signals were detected using the FUJIFILM Luminescent Image Analyzer LAS-4000mini (FUJIFLIM Corporation, Tokyo, Japan).

7. Western blotting

Total protein was extracted from 25 mg of infiltrated leaves that were ground in liquid nitrogen in a motor and pestle and suspended in 250 µl of 1% SDS-PAGE Laemmli's sample buffer (0.5 M Tris-HCl pH 6.8, 10% glycerol, 5% mercaptoethanol, 1% SDS, 0.01% Bromophenol blue). The mixture was vortexed and denatured at 95°C for 5 min. It was centrifuged at 14000 rpm for 5 min at 4℃. 10 µl of each sample was loaded in the well in SDS-PAGE gel and ran for 40 minutes (0.3 A per gel). A PVDF membrane was prepared and replaced with a transformation buffer along with filter paper. Three sheets of filter paper, gel, PVDF membrane, and three sheets of filter paper were stacked on top of each other in order from the bottom to the bottom on a blotting device and transferred at 15V for 30 minutes. After transfer, the gel was shaken and stained with CBB and decolorized solution. The transferred PVDF membrane was soaked in Blocking buffer (TBST buffer + 5% skim milk) and allowed to stand on shaker for an hour. The primary antibody (diluted 1000 times) was added to TBST-T buffer + 5% skim milk solution and allowed to stand on shaker for 35 min. The solution was discarded and washed three times with ELiX, followed by TBST-T wash three times 5 min each and TBST wash one time for 5 minutes on the shaker. The secondary Goat AP-antibody-IgG was added to TBST-T buffer + 5% skim milk solution and allowed to stand on shaker for 45 min. The solution was discarded and washed

once with ELiX, followed by TBST wash four times 5 min each on the shaker. PVDF membrane with 1 ml of AP buffer (100 mM Tris-HCl pH 9.5, 100 mM NaCl, 5 mM MgCl2) and 5µl of CDP-Star were packaged using a sealer, and the protein signal was detected using LAS-4000 mini.

8. Total RNA extraction

Total RNA was extracted using TRIzol Reagent (Thermo Fisher Scientific, Waltham, MA, USA). 50 mg of infiltrated leaf tissue was collected at 3 days post-infection (dpi) and crushed in liquid nitrogen. 1 ml Trizol was added, vortexed and incubated for 5 min in room temperature. 100 µl of Chloroform was added and the mixture was vortexed for 5 min. It was incubated for 3 min and centrifuged at 14000 rpm for 15 min at 4℃. The aqueous phase was transferred into a new Eppendorf tube. 250 µl of 2-propanol was added, inverted and incubated for 10 min in room temperature. It was centrifuged at 14000 rpm for 15 min at 4℃ and the supernatant was discarded. 1 ml of 70% ethanol was added and centrifuged at 14000 rpm for 3 min. The supernatant was discarded and air dried for 5 min. 200 µl of RNase-free water, 100 µl of Phenol and 100 µl of chloroform were added and the mixture was vortexed for 5 min. It was centrifuged at 14000 rpm for 15 min at 4℃. The aqueous phase was transferred into a new tube and 2.5 times of 100% ethanol, and 1/10th volume of NaAc was added. It was inverted and centrifuged at 14000 rpm for 15 min. The supernatant was discarded, and 1 ml 70% ethanol was added. It was centrifuge at 14000 rpm for 3 min at 4℃. The supernatant was discarded and air dried for 5-10 min. It was resuspended with 50 µl of D.W. and stored at -80℃. The RNA concentration was checked by NanoDrop.

9. cDNA preparation

A total of 25 µl of RNA was mixed with, 3 µl of 10× DNase1 incubation buffer, 1 µl of DNase1, and 0.5 µl of RNase inhibitor and incubated at 37℃ for 30 min. 200 µl nuclease-free water, 100 µl of phenol, and 100 µl of chloroform (100 µl each) was added. The mixture was vortexed for 1 min and then centrifuged at 14000 rpm for 3 min. 200 µl of supernatant was transferred into a new Eppendorf tube. $1/10^{th}$ volume (20 µl) of 3 M sodium acetate (pH 5.0) and 2.5 times of volume (500 µl) of 100% ethanol was added and vortexed. It was centrifuged at 14000 rpm for 5 min and the supernatant was discarded. 1 ml of 70% ethanol was added and centrifuged at 14000 rpm for 3 min. The supernatant was discarded, and the pellet was air-dried for 5-10 min. The pellet was resuspended in 25 µl of nuclease-free water, and boiled to denature for 2 min.

Reverse transcription was carried out using ReverTra Ace® reverse transcriptase (Toyobo Co., Ltd., Osaka, Japan) reagents according to the manufacturer's instructions. The reaction mixture was prepared by adding the reagents in the **Table 6**, and then incubated at 30℃ for 10 min, 42℃ for 30 min, and 99℃ for 5 min.

Table 6: Reverse transcription mixture solution.

Reagents	**Volume (20 µl)**
Denatured total RNA	2–3 µl (0.5–5 µg)
Random hexamer primers	0.5 µl
5× reverse transcription buffer	4 µl
10 mM dNTP	2 µl
RNase inhibitor	0.5 µl
ReverTraAce reverse transcriptase (Toyobo Co., Ltd., Osaka, Japan)	1 µl
Nuclease-free water	up to 20 µl

10. Quantitative RT-PCR

Quantitative RT-PCR mixture was prepared by adding the reagents in **Table 7**. The forward and reverse primers were designed from the NCBI database sequences for eIF4E1/9DEL-eIF4E1, R2b, GFP and the NbL23areal (used as a positive control) are listed in **Table 8**. The qRT-PCR was performed using the conditions listed in **Table 9**.

Table 7: Quantitative RT-PCR mixture reagents.

Reagents	Volume (10 µl)
Thunderbird® Next SYBR™ qPCR Mix (Toyobo Co., Ltd., Umeda, Osaka, Japan)	5 µl
Forward primer	0.15 µl
Reverse primer	0.15 µl
cDNA	1 µl
Nuclease-free water	up to 10 µl

Table 8: Quantitative RT-PCR primers.

Primer name	Sequence
eIF4E1-Forward	5′-ATGGAACAGAAACTGATCTCTGAAG-3′
eIF4E1-Reverse	5′-AGTTCATCGTCTACCTCTCCTCCTC-3′
R2b- Forward	5′-ATGGAATTGAACGTAGGCGCGATGA-3′
R2b-Reverse	5′-ACTTTTGTGACCTCGTTCCCGTCGA-3′
GFP-Forward	5′-ATGAGTAAAGGAGAAGAACTTTTCAC-3′
GFP-Reverse	5′-TCCGTATGTTGCATCACCTTCACCC-3′
NbL23areal-Forward	5′-CATTGTTGATCTCAAAGCTGACAAG-3′
NbL23areal-Reverse	5′-GAACAAACGCCTTCTTGGTTCCATC-3′

Table 9: Quantitative RT-PCR amplification conditions.

Starting		Denaturation	Annealing	Extension	Post-cycling stage		
95°C	40 Cycles	94°C	60°C	72° C	95°C	65°C	95°C
2 min		5 sec	10 sec	40 sec	30 sec	30 s	30 sec

11. Inoculation test

The plants were treated with 1mM BTH (benzothiadiazole) to induce SA plant defense 1 day before inoculation. 3 ml of inoculation buffer (0.1 M phosphate buffer, pH 7.0 and 1% of total volume of Mercaptoethanol) was added to grind the CMV-Y, CMVΔ2b (lacking 2b), and CMV-2bΔC (truncated C-terminus of 2b) infected *N. benthamiana* leaves. Carborundum powder was sprinkled on the leaves of tomato 'S8' and *9DEL* seedlings at the second or third true leaf stage. The inoculum was wiped on the leaves using a cotton bud and washed out with distilled water. Uninoculated plants were used as healthy controls. The infection was observed, and the leaves were harvested at 35 days post inoculation.

Mean and SE of absorbance values at 405 nm of samples from at least six independent plants per genotype were calculated. The susceptibility threshold was set as 3× the mean value of healthy controls.

12. ELISA test

At 35 dpi, CP accumulation in uninoculated upper leaves was investigated with anti-CP polyclonal antibody in a double antibody sandwich enzyme-linked immunosorbent assay (DAS-ELISA). 200 µl of 0.05 M carbonate-bicarbonate buffer (1 volume of 0.05 M Na2CO3 and 3 volumes of 0.05 M NaHCO3; pH to 9.6) with 1,000 times diluted anti-CMV CP polyclonal antibody was dispensed into each well of a micro-plate and incubated at 37℃ for 2 hours to coat (immobilize through hydrophobic interactions). Then the solution was discarded. 200 µl of PBS-T (137 mM NaCl, 8.1 mM Na2HPO4.12H2O, 1.47 mM KH2PO4, 2.7 mM KCl, 0.05% Tween20, (NaN3 0.2g/L)) wash buffer was added and discarded after 5 minutes. This washing step was repeated 3 times. 1 ml of PBS-T buffer (10 times to leaf weight) was added, and the harvested leaf crude was extracted. It was

vortexed and centrifuge at 14,000 rpm for 10 min at 4℃. 200 µl of the supernatant was added to the wells (2 repeats for each sample). It was incubated overnight at 4℃. Then the solution was discarded, and the PBS-T washing was repeated. 200 µl of PBS-T with 1,000 times dilute AP-labeled anti-CMV CP polyclonal was dispensed into each well and incubated at 37℃ for 1 hour. Then the solution was discarded, and the PBS-T washing was repeated. 200 µl of 10% diethanolamine aqueous solution (pH 9.8 adjusted with HCl) with 0.2-0.3% disodium para-nitrophenyl phosphate hexahydrate (60 mg/0.06g) dissolved was dispensed into each well to develop color. It was incubated at room temperature and the absorbance value was measured.

Chapter I

Identification of interaction between the genome-edited in-frame mutant of eIF4E1 (9DEL) and CMV-2b

Introduction

The development of virus-resistant crops is a cornerstone of sustainable agriculture. Traditional resistance breeding relies on the use of naturally occurring recessive resistance alleles, particularly those affecting susceptibility genes such as *eIF4E*, *eIF4G*, and their isoforms, which are essential for viral replication and movement. Loss-of-function mutations in the *eIF4E* gene have been exploited to develop resistance against a wide range of viruses, especially potyviruses (**Piron et al., 2010; Gauffier et al., 2016**).

Plant-virus interactions involve a dynamic interplay between host defense mechanisms and viral strategies aimed at overcoming host defense. One of the pivotal targets in this molecular interplay is the host eukaryotic translation initiation factor 4E (eIF4E), which is not only essential for mRNA translation but also frequently co-opted by plant RNA viruses for their replication and infection processes (**Bastet et al., 2017**). In tomato (*Solanum lycopersicum* L.), the eIF4E1 protein has emerged as a critical host susceptibility factor, particularly for positive-sense RNA viruses such as Cucumber mosaic virus (CMV).

Traditional resistance breeding targeting *eIF4E* alleles has provided durable resistance in many crops. However, these strategies often introduce linkage-drag undesirable traits or limitations in resistance durability. Genome editing technologies such as CRISPR/Cas9 have now enabled the generation of precise, transgene-free modifications in susceptibility genes. Instead of complete knockouts, which may disrupt plant development, in-frame deletions are emerging as an effective approach to confer resistance while maintaining protein functionality (**Chandrasekaran et al., 2016; Bastet et al., 2019**).

In this context, a novel allele of tomato eIF4E1 (*9DEL*) was generated by in-frame deletion of nine amino acids in a region suspected of mediating interaction with viral proteins. Previous studies have shown that plants harboring the *9DEL* allele retain normal growth and yet exhibit partial resistance to CMV infection, which is absent in *1INS* knockout plants or wild-type 'S8' tomato (**Atarashi et al., 2020**). Notably, this mutant allele does not confer resistance to PVY, suggesting a CMV-specific resistance mechanism. This observation led to the hypothesis that mutant eIF4E1 from *9DEL* may interact with CMV proteins in a mutation-specific manner.

CMV is one of the most widespread and economically damaging plant viruses. Its genome comprises three RNA segments, with RNA2 encoding the 2b protein translated from the sub-genomic RNA4A, a well-characterized viral suppressor of RNA silencing (VSR) (**Zhang et al., 2006**). The 2b protein counteracts antiviral RNA interference (RNAi) by binding small RNAs and interacting with AGO proteins, thereby inhibiting the RNA-induced silencing complex (RISC) and suppressing post-transcriptional gene silencing (**González et al., 2010**). This function is critical for CMV pathogenicity and systemic movement within the plant. In addition, 2b modulates plant defense signaling by interfering with salicylic acid (SA) and jasmonic acid (JA) pathways, contributing to systemic movement and symptom induction (**Lewsey et al., 2009; Zhang et al., 2024**). Importantly, 2b contains a highly variable C-terminal region that determines its subcellular localization and interactions with host proteins. Strain-specific polymorphisms, such as those found in HL2b, R2b, and Y2b variants, affect symptom severity and binding affinity to host proteins (**Goto et al., 2007; Sueda et al., 2010**). Given the essential role of 2b in CMV infection

and the sequence variability among its isoforms, 2b was selected as a candidate for interaction analysis, potentially contributing to CMV-specific resistance mechanisms.

Therefore, this chapter focuses on investigating the physical interaction between 9DEL-eIF4E1 and the CMV proteins using protein-protein interaction assays. To address this, I employed yeast two-hybrid (Y2H), split-luciferase complementation, and subcellular co-localization assays. These complementary approaches allow to assess direct interaction between two proteins in vitro and in planta.

Results

1. eIF4E1 and 9DEL both interact with CMV 2b protein in Y2H assay

The 9-nucleotide in-frame deletion (*9DEL*) in eIF4E1 enhances CMV resistance, unlike the out-of-frame *1INS* frameshift mutation (**Atarashi et al., 2020**), suggesting that the resistance-associated with *9DEL* mutant protein may interfere with specific CMV viral proteins during infection. To investigate this hypothesis, I conducted yeast two-hybrid (Y2H) assay to identify the protein-protein interactions between eIF4E1 or 9DEL-eIF4E1 protein and key CMV proteins. In the initial screening, I evaluated CMV proteins: coat protein (CP), movement protein (MP), and RNA silencing suppressor protein 2b, which is a critical target in host antiviral defense strategies. I selected distinct 2b protein variants from two different CMV strains R2b, and HL2b, for interaction with eIF4E1 and 9DEL-eIF4E1. R2b isoform derived from strain CM95R (a subgroup I isolate), is known for its potent RNA silencing suppressor (RSS) activity and has been shown to be highly virulent in model plants such as *Arabidopsis thaliana* and *Nicotiana benthamiana* (**Goto et al., 2007**). Its strong nuclear localization and broad-spectrum suppression of post-transcriptional gene silencing (PTGS) make it an ideal representative of fully functional 2b proteins. While the HL2b isoforms, derived from CMV-HL lily isolate (also a subgroup I isolate), represent a functionally attenuated 2b protein. Previous studies show HL2b exhibits weaker silencing suppression, altered nuclear localization, and lower toxicity to E. coli (**Sueda et al., 2010; Masuta et al., 2012**), suggesting it has reduced affinity for host silencing components. Importantly, HL2b serves as a negative control variant, allowing us to test whether reduced virulence correlates with a loss of eIF4E1 interaction. Including

HL2b provides a mechanistic comparison point for understanding which 2b residues are essential for eIF4E1 binding. These 2b variants encompasses the functional spectrum of CMV 2b proteins, ranging from strong (R2b) to weak (HL2b) silencing suppressors. Yeast cells co-expressing either wild-type eIF4E1 or 9DEL-eIF4E1 interacted with the R2b protein demonstrated growth on selective quadruple-dropout (QDO) medium (**Figure 1a**). But no interaction was observed between eIF4E1 or 9DEL-eIF4E1 with CMV CP and MP, as confirmed by lack of growth on QDO medium (**Figure 1a**). I also evaluated Y2b from CMV-Y isolates, nearly identical in sequence to Fny2b, which is the most extensively studied 2b protein in *Arabidopsis* and *Nicotiana* (**Zhang et al., 2006; Lewsey et al., 2009**). Y2b is known to bind AGO1, suppress RNA silencing, and induce strong symptoms, making it an excellent comparator to R2b for validating reproducibility across highly active 2b variants. Including Y2b helps to demonstrate whether interaction patterns observed with R2b are conserved in other functionally equivalent 2b proteins. Y2b also demonstrated interaction with eIF4E1 and 9DEL-eIF4E1 in Y2H (**Figure 1b**), while HL2b failed to interact (**Figure 1a**), differs from R2b and Y2b in several biochemical and biological properties, including lower toxicity to *E. coli* (**Goto et al., 2007; Sueda et al., 2010**). Fny2b (from CMV-Fny) is therefore expected to interact similarly with eIF4E1 and 9DEL-eIF4E1. I aligned the amino acid sequence and showed that HL2b possesses unique amino acid substitutions to R2b and Y2b at five positions (**Figure 1c**), which helps to explain its inability to interact with eIF4E1 and 9DEL-eIF4E1. The substitutions are dispersed throughout the 2b coding region. Thus, identifying which residues are responsible for difference in the binding affinity could reveal the essential regions within 2b for eIF4E1 interaction. To examine this, point mutants were generated to substitute the five amino acid

residues in R2b with the corresponding residues from HL2b (**Figure 1d**). The Y2H result demonstrated that substitutions at residues 94 and 104 in the C-terminal region of R2b mutants resulted in complete loss of interaction with both eIF4E1 and 9DEL-eIF4E1. Conversely, introducing the reciprocal substitutions at residues 94 and 104 into HL2b mutants restored its ability to interact with eIF4E1 variants (**Figure 1d**), suggesting that the C-terminal region of 2b, particularly residues 94 and 104, is critical for the interaction with eIF4E1 proteins.

2. **Confirmation of interaction of eIF4E1 and 9DEL-eIF4E1 with 2b protein using split-luciferase complementation assay and subcellular co-localization test in planta**

In the previous experiments, yeast two-hybrid (Y2H) assays demonstrated that both wild-type eIF4E1 and its in-frame mutant 9DEL-eIF4E1 interact with CMV 2b variants (R2b and Y2b) in vivo. To independently validate the interactions in planta, I employed a split-luciferase complementation assay in *Nicotiana benthamiana*. R2b was fused to either the N-terminal (nLUC) or C-terminal (cLUC) fragment of luciferase, while eIF4E1, 9DEL-eIF4E1, and the coat protein (CP) of potato virus X (PVX), were fused to the complementary luciferase fragment (**Figure 2**). PVX (Potato virus X) belongs to the genus *Potexvirus* (family *Alphaflexiviridae*) was used as a negative control. PVX is phylogenetically and functionally unrelated to CMV and lacks a 2b homolog or silencing suppressor. Its coat protein (CP) does not hijack host translation factors and has been widely used as a neutral, non-interacting control in split-LUC assay **(Chen et al., 2008b; Horstman et al., 2014)**. I carried out *Agrobacterium*-mediated infiltration in *N. benthamiana* leaves to co-express these fusion constructs transiently (**Figure 2**). Protein-protein interaction between the infiltrated pairs was detected by chemiluminescent signals produced upon luciferase reconstitution, which occurs only when the interacting partners bring the luciferase fragments into close proximity. Strong and reproducible chemiluminescent signals were detected in leaf areas co-expressing R2b with either eIF4E1 or 9DEL-eIF4E1, indicating that both proteins physically interact with R2b in planta (**Figure 2**). In contrast, no luminescence was observed when R2b was co-expressed with the negative control PVX CP, confirming the specificity of the interaction. Notably,

consistent with previous reports of 2b homodimerization (**Chen et al., 2008b**), a robust luminescent signal was also observed in tissues co-expressing R2b fused separately to both nLUC and cLUC, serving as an internal positive control (**Figure 2**). These results indicate that both eIF4E1 and 9DEL-eIF4E1 proteins interact with CMV R2b within the plant cells, supporting the protein-protein interaction previously observed in Y2H.

To further confirm the interaction of 2b with eIF4E1 and 9DEL-eIF4E1 in planta, I conducted a subcellular co-localization analysis using confocal microscopy. Constructs expressing 2b fused to GFP and eIF4E1 or 9DEL-eIF4E1 fused to dsRed were transiently co-expressed in *Nicotiana benthamiana* via *Agrobacterium*-infiltration. Fluorescence microscopy revealed that GFP-2b was localized to both nucleus and cytoplasm, with particularly strong signals observed at the nucleus and cytoplasm (**Figure 3**), consistent with its previously reported cellular localization (**Zhang et al., 2006; Lewsey et al., 2010**). In contrast, dsRed-eIF4E1 and dsRed-9DEL-eIF4E1 were localized primarily in the cytoplasm, with faint but detectable nuclear signals, reflecting their role in cap-dependent cytoplasmic mRNA translation. Merged fluorescence images showed an extensive overlap between the GFP-2b and dsRed-eIF4E1 or dsRed-9DEL-eIF4E1, producing strong yellow signals, particularly at perinuclear and cytoplasmic regions, indicating co-localization between 2b and both eIF4E1 variants (**Figure 3**). To ensure that this overlap was not because of nonspecific distribution or overexpression, a series of negative controls were included: GFP-2b co-expressed with empty dsRed, and dsRed-eIF4E1 or dsRed-9DEL-eIF4E1 co-expressed with empty GFP, and independent expression of each construct. These controls showed no overlapping fluorescence signals, confirming the specificity of the observed co-localization (**Figure 3**). Collectively, these results support that 2b and both

eIF4E1 and 9DEL-eIF4E1 co-localized within the same cellular compartments in planta, reinforcing the likelihood of a biologically relevant physical interaction, and supporting the hypothesis that 9DEL-eIF4E1 may functionally interfere with 2b function through direct spatial association.

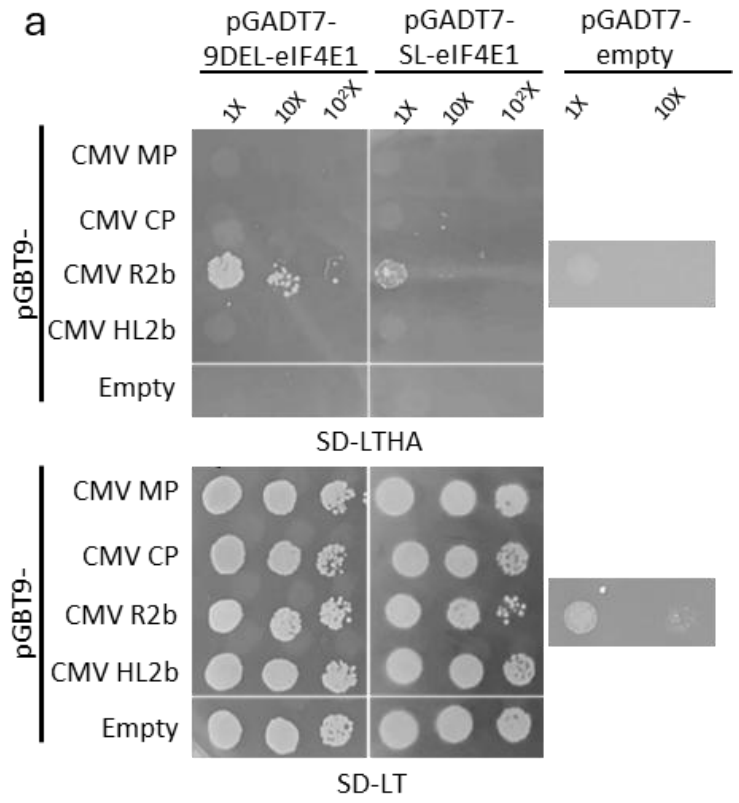
a
pGADT7-9DEL-eIF4E1
pGADT7-SL-eIF4E1
pGADT7-empty
1X
10X
10^2X
1X
10X
10^2X
1X
10X
pGBT9-
CMV MP
CMV CP
CMV R2b
CMV HL2b
Empty
SD-LTHA
pGBT9-
CMV MP
CMV CP
CMV R2b
CMV HL2b
Empty
SD-LT

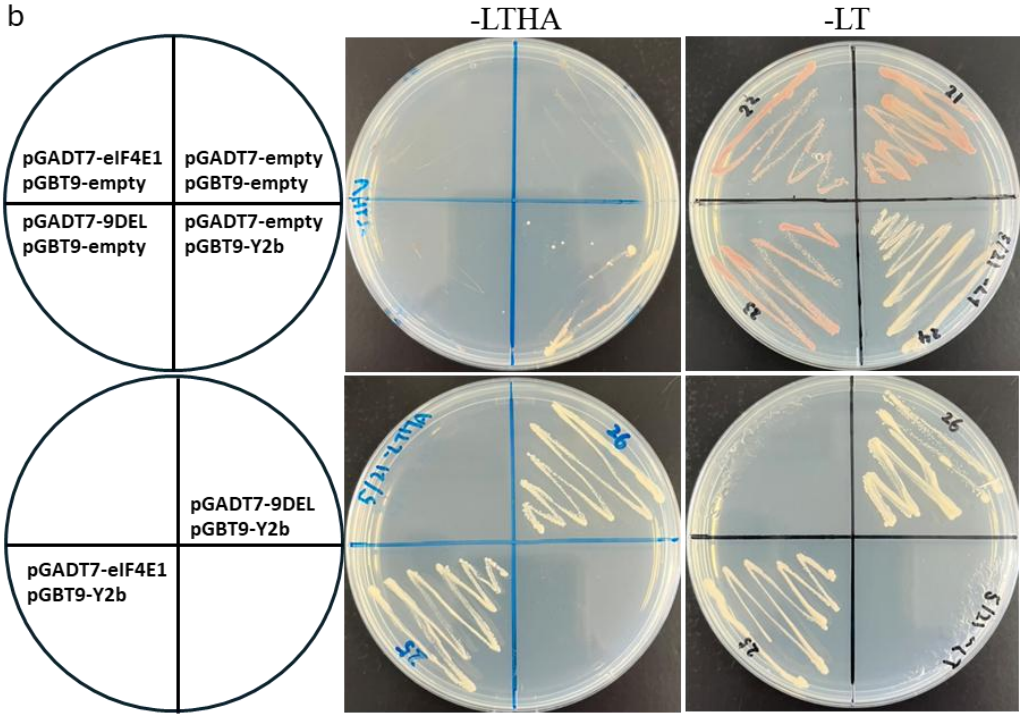
b
-LTHA
-LT
pGADT7-eIF4E1
pGBT9-empty
pGADT7-empty
pGBT9-empty
pGADT7-9DEL
pGBT9-empty
pGADT7-empty
pGBT9-Y2b
pGADT7-9DEL
pGBT9-Y2b
pGADT7-eIF4E1
pGBT9-Y2b

c

```
Y2b    MELNVGAMTNVELQLARMVEAKKQRRRSHKQNRRERGHKSPSERARSNLRLFRFLPFYQV
R2b    MELNVGAMTNVELQLARMVEAKKQRRRSHKQNRRERGHKSPSERARSNLRLFRFLPFYQV
HL2b   MELNAGAMTNVELQLARMVEAKRQRRRSHKQNRRERGHKSPSERARSNLRLFRFLPFFQV

Y2b    DGSELTGSCRHANVAESPEPEASRLELSAEDHDFDDTDWFAGNEWAEGAF
R2b    DGPELTGSCRHVNVAELPEPEASRLELSAEDHDFDDTDWFAGNEWAEGTF
HL2b   DGSELTGSCRHMNVAELPEPEASRLELSAEDHDLDDTDWFAGNKWAEGAF
```

d

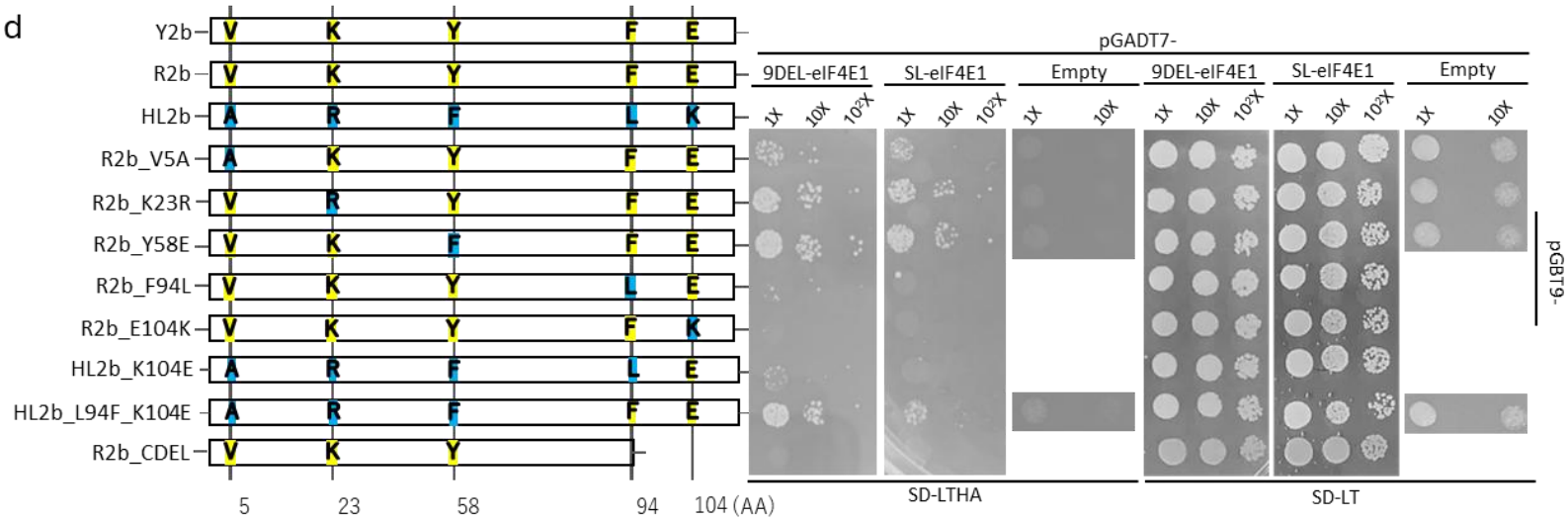

Figure 1: Interaction of CMV R2b with eIF4E1 and 9DEL-eIF4E1 in yeast two-hybrid (Y2H) assay. (a) Yeast two-hybrid analysis was performed to examine the interactions between wild-type eIF4E1 and 9DEL-eIF4E1 mutant with various CMV proteins, including coat protein (CP), movement protein (MP), R2b (from CMV-R95), and HL2b (from CMV-HL). Constructs were cloned into pGADT7 (eIF4E1 and 9DEL-eIF4E1) and pGBT9 (CMV viral proteins) vectors and co-transformed into *Saccharomyces cerevisiae* strain Y2H Gold. Protein-protein interactions were assessed based on yeast growth on selective media (SD–Leu–Trp and SD–Leu–Trp–His–Ade). Interaction was confirmed by robust growth of yeast co-expressing R2b with either eIF4E1 or 9DEL-eIF4E1, while no interaction was observed with CP, MP, and HL2b. (b) Y2H interaction assay with Y2b (from CMV-Y) showed clear interaction with both eIF4E1 and 9DEL-eIF4E1, as evidenced by strong growth on SD–LTHA media, supporting a specific interaction. While Y2b showed slight self-activation, as indicated by weak growth when co-expressed with an empty vector, the interaction with eIF4E1 or 9DEL-eIF4E1 was clearly stronger. (c) Amino acid sequence alignment of Y2b, R2b, and HL2b proteins reveal five amino acid substitutions that distinguish HL2b from R2b or Y2b. Key substitutions residues conserved between Y2b and R2b are highlighted in yellow, and HL2b-unique substitutions are shown in blue. (d) Schematic diagram of targeted point mutations in R2b and HL2b constructs used to assess the essential residues responsible for interaction with eIF4E1 variants. Eight mutant variants were generated by point mutations and tested in Y2H assays. Substitution of residues 94 and 104 in R2b abolished interaction with eIF4E1 and 9DEL-eIF4E1, while reciprocal substitution into HL2b restored binding, highlighting these C-terminal residues as key determinants for binding. Assays were repeated thrice for consistency.

	cLUC	nLUC
1	R2b	PVX CP
2	9DEL-eIF4E1	R2b
3	9DEL-eIF4E1	PVX CP
4	R2b	R2b
5	eIF4E1	R2b
6	eIF4E1	PVX CP

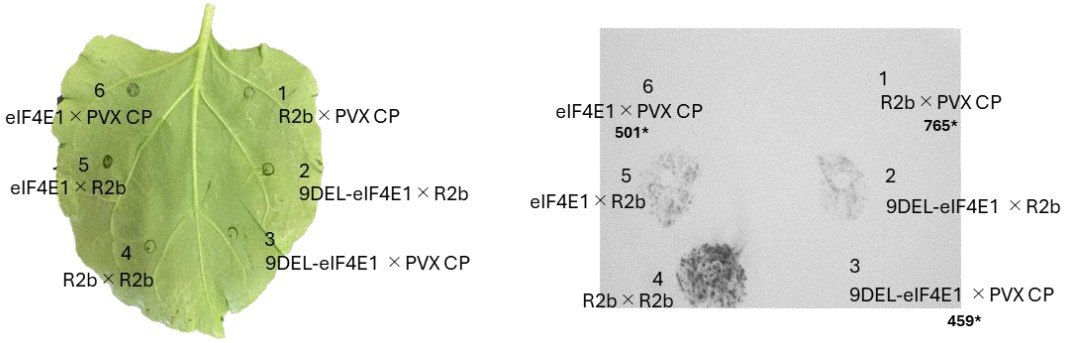

Figure 2: Confirmation of R2b interaction with eIF4E1 and 9DEL-eIF4E1 using a split-luciferase complementation assay. Agrobacterium-mediated transient expression was used to co-infiltrate *N. benthamiana* leaves with constructs encoding luciferase fragments fused to the targeted proteins (PVX CP and R2b fused to N- and R2b, eIF4E1, and 9DEL-eIF4E1 to C-terminal). Reconstitution of luciferase activity, indicated by chemiluminescent signal, reflects protein-protein interaction in planta. Chemiluminescence images were detected at 2 dpi using LAS-4000mini. Quantitative luminescence (integrated density) was measured using ImageJ software, values are marked with an asterisk (*). Luminescence indicates interactions between the co-expressed proteins. Strong luminescence was detected in leaf sectors co-expressing R2b with eIF4E1 or 9DEL-eIF4E1, confirming their physical interaction. Notably, R2b–eIF4E1 exhibited higher luminescence than R2b-9DEL. Self-interaction of R2b (R2b-nLUC + R2b-cLUC) served as a positive control. In contrast, PVX CP combinations produced minimal luminescence, confirming the specificity of the interaction. Assays were repeated three times with consistent results.

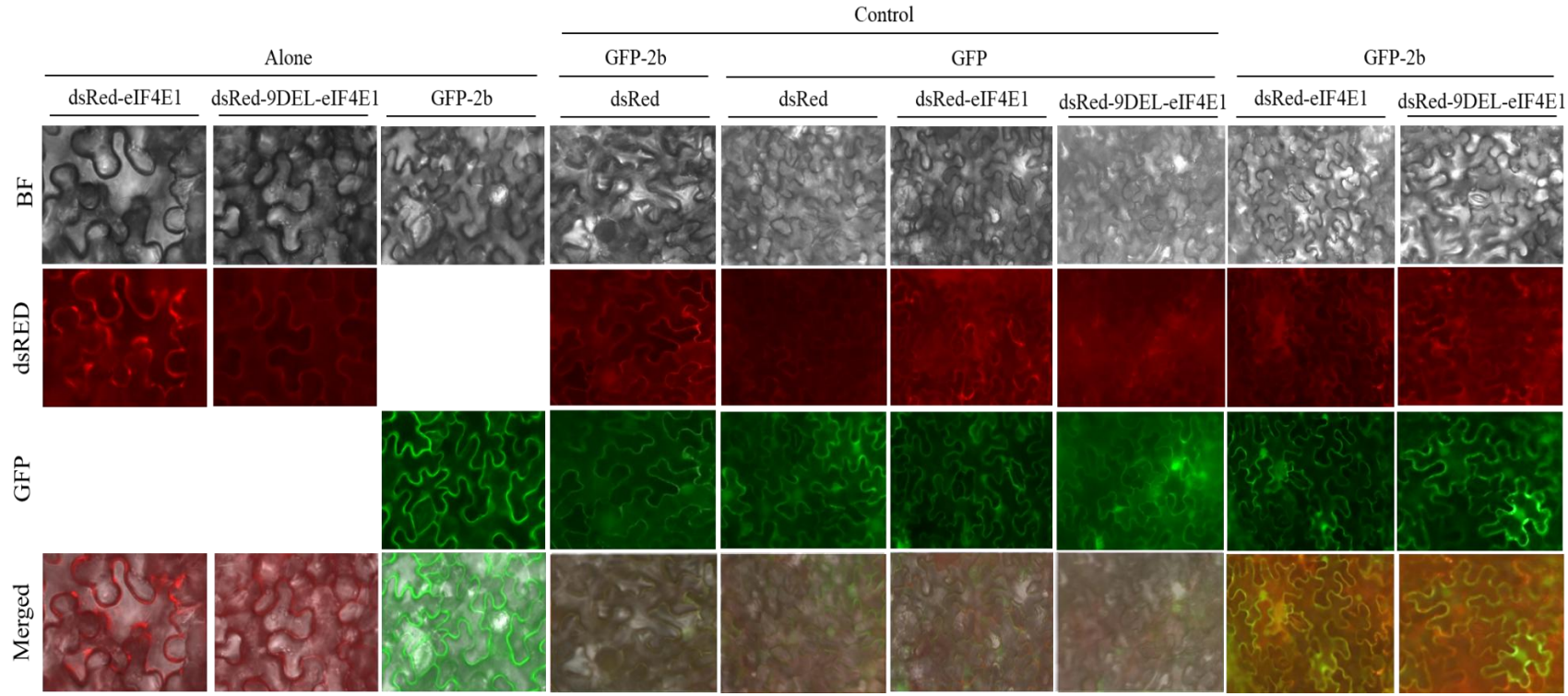
Control
Alone
GFP-2b
GFP
GFP-2b
dsRed-eIF4E1
dsRed-9DEL-eIF4E1
GFP-2b
dsRed
dsRed
dsRed-eIF4E1
dsRed-9DEL-eIF4E1
dsRed-eIF4E1
dsRed-9DEL-eIF4E1
BF
dsRED
GFP
Merged

Figure 3: Subcellular co-localization of CMV 2b with eIF4E1 and 9DEL-eIF4E1 in *Nicotiana benthamiana*. Confocal microscopy of Agrobacterium-infiltrated *N. benthamiana* epidermal cells at 4 dpi co-expressing GFP-2b with dsRed-eIF4E1 or dsRed-9DEL-eIF4E1 showed that 2b localized to both the nucleus and cytoplasm, while both eIF4E1 variants were primarily cytoplasmic with weaker nuclear signals. Merged images revealed yellow fluorescence in co-expressing cells, indicating subcellular co-localization, especially in perinuclear and cytoplasmic regions. Negative controls- GFP-2b with empty dsRed, dsRed-eIF4E1 or dsRed-9DEL-eIF4E1 with empty GFP, and independent expression of each construct, showed no fluorescence overlap, confirming the specificity of the observed co-localization. These findings suggest that 2b and both eIF4E1 variants occupy overlapping subcellular domains, supporting the possibility of physical interaction in planta.

Discussion

Plant resistance to viruses often depends on two primary mechanisms: dominant resistance (R) genes or recessive loss-of-function mutations in host susceptibility factors. Among these, the eukaryotic translation initiation factor 4E (eIF4E) gene family has emerged as a major reservoir for recessive resistance to several RNA viruses (**Zhou et al., 2014; Bastet et al., 2017; Zlobin & Taranov, 2023**). Natural or engineered mutations in eIF4E often disrupt their interaction with viral proteins like VPg, interrupting the viral life cycle by impairing the function of this susceptibility factor essential for infection and replication **(Zhou et al. 2014; Gao et al. 2018; Zhao et al. 2018; Shukla et al. 2020; Yoon et al. 2020; Yu et al. 2020**). A loss-of-function eIF4E mutant in Arabidopsis confers recessive resistance to CMV by preventing the virus from exploiting the host factor, with resistance observed only in homozygous individuals lacking the wild-type allele (**Yoshii et al., 2004**). Notably, such mutations often confer sustainable, broad-spectrum resistance without compromising essential host functions (**Piron et al., 2010**).

While most studies on eIF4E-mediated resistance focus on potyviruses, whose VPg directly recruits eIF4E to initiate cap-independent translation, fewer studies have addressed its role in non-VPg-dependent viruses, like cucumber mosaic virus (CMV). CMV encodes the 2b protein, a multifunctional RNA silencing suppressor that antagonizes the host RNAi machinery by binding siRNAs and AGO proteins (**Zhang et al., 2006; Lewsey et al., 2010**). This suppressor is essential for systemic infection, virulence, and suppression of host defense pathways. However, natural plant alleles that inhibit 2b function are rare, and the mechanistic understanding of host proteins that can neutralize 2b is limited.

In this context, I investigated whether a previously characterized CRISPR/Cas9-edited in-frame deletion mutant of tomato eIF4E1 (*9DEL*), which confers partial CMV resistance (**Atarashi et al., 2020**), might interact with CMV viral proteins and interfere with CMV infection and replication. Interestingly, plants with a frameshift mutation (*1INS*) completely abolished eIF4E1 function are more susceptible than *9DEL* plants. This suggests that resistance in *9DEL* is not a result of a loss-of-function but a gain-of-function trait that interferes with CMV proliferation.

To test this hypothesis, whether 9DEL-eIF4E1 physically interacts with viral proteins to mediate this resistance, I screened eIF4E1 and 9DEL-eIF4E1 against key CMV proteins: coat protein (CP), movement protein (MP), and three 2b variants (R2b, Y2b, HL2b) using yeast two-hybrid (Y2H) assays. The interaction was specific to the R2b (**Figure 1a**) and Y2b (**Figure 1b**) protein from the CMV subgroup I isolate, while the HL2b variant, which carries five unique amino acid changes (**Figure 1c**), failed to interact (**Figure 1a**). Site-directed mutagenesis revealed that substitutions at residues 94 and 104 in the C-terminal domain of 2b were critical for interaction with both eIF4E1 and 9DEL-eIF4E1 (**Figure 1d**). This is consistent with prior evidence that the C-terminal domain of 2b affects its interaction with host proteins and suppressor function (**Goto et al., 2007; Sueda et al., 2010**). However, the 9-amino acid deletion in *9DEL* does not disrupt this interaction, suggesting that the partial resistance in *9DEL* plants is not caused by loss of binding, but is likely due to a functional change in the resulting protein expression.

To verify this result, I used split-luciferase complementation assays in *Nicotiana benthamiana* and observed reconstitution of luciferase signals when R2b was co-expressed with either eIF4E1 or 9DEL-eIF4E1 (**Figure 2**), confirming a physical interaction in planta.

Control combinations with PVX coat protein failed to yield signal, demonstrating specificity. Importantly, the result also replicated the known self-interaction (homo-dimerization) of 2b, as reported previously (**Chen et al., 2008b**). Further, subcellular co-localization analysis revealed that 2b was localized to both the nucleus and cytoplasm, aligning with its dual role in transcriptional and post-transcriptional silencing suppression (**Lewsey et al., 2010; Wu et al., 2017**). eIF4E1 and 9DEL-eIF4E1 were primarily cytoplasmic, with occasional nuclear signals. Co-expression of GFP-2b with dsRed-eIF4E1 and dsRed-9DEL-eIF4E1 showed extensive cytoplasmic co-localization, particularly near the nuclear periphery (**Figure 3**). This spatial overlap reinforces the likelihood of functional interaction, potentially allowing 9DEL-eIF4E1 to destabilize 2b in a manner not achievable by wild-type eIF4E1. This spatial overlap supports the possibility of a functional interaction, suggesting that 9DEL-eIF4E1 may interfere with 2b function in a way that cannot be achieved by wild-type eIF4E1. Taken together, the results provide the first direct evidence that eIF4E1 interacts with the CMV 2b protein. While the *9DEL* mutation does not disrupt this interaction but may instead interfere with the functional outcome of this interaction, supporting a gain-of-function resistance mechanism. This extends the antiviral role of eIF4E1 beyond its established interactions with VPg and highlights the potentiality of precise in-frame deletions, rather than full knockouts, as a novel approach to impair the function of viral suppressors.

Chapter II

Functional significance of 2b inhibition by genome-edited eIF4E1 (9DEL) in CMV resistance

Introduction

Developing virus-resistant crops is a major objective in modern agriculture, especially in combatting RNA viruses. The challenge of engineering virus-resistant crops is urgent like Cucumber mosaic virus (CMV), an RNA virus with one of the broadest host ranges among plant viruses. CMV infects numerous economically important crops such as tomato, cucumber, melon, pepper, and tobacco, causing serious yield losses worldwide. Traditional resistance breeding often targets viral replication or movement proteins, but CMV presents a unique challenge because of its potent viral suppressor of RNA silencing (VSRs), which actively disrupts host defense mechanisms (**Garcia-Ruiz, 2018; Ghoshal & Sanfaçon, 2015**).

Plant antiviral defense systems rely on a multilayered framework that includes both innate immune responses and post-transcriptional gene silencing (PTGS). Among which RNA silencing is the most critical. This defense is initiated by Dicer-like (DCL) proteins that process viral double-stranded RNA into small interfering RNAs (siRNAs), which are then incorporated into ARGONAUTE (AGO) proteins within the RNA-induced silencing complex (RISC) to target viral RNA for degradation (**Liu et al., 2022; Zhao et al., 2023; Huang et al., 2025**). CMV's 2b protein undermines this system by directly binding both siRNAs and AGO1, neutralizing RISC and facilitating infection (**Zhang et al., 2006; González et al., 2010**). In addition, 2b interferes with transcriptional gene silencing by altering DNA methylation and fibrillarin localization, weakening systemic immunity (**Lewsey et al., 2010; Garcia-Ruiz, 2018**).

Besides 2b's critical role in CMV pathogenicity, no natural resistance gene has been found in tomatoes or other crops that directly target 2b. Instead, CMV resistance is often polygenic and derived from wild relatives such as *Solanum habrochaites* and *Capsicum annuum*, where resistance correlates with enhanced RNA silencing activity or elevated expression of genes like *AGO1* and *DCL2* (**Caranta et al., 2002; Li et al., 2020; Akhter et al., 2021**). Recent innovations such as artificial microRNAs and peptide decoys have explored ways to suppress VSRs, but practical deployment remains limited (**Zhang et al., 2011**).

A promising strategy for developing virus resistance lies in susceptibility genes like *eIF4E1*. eIF4E1 is traditionally known for its role in translation initiation, a well-established target of VPg proteins of potyviruses, and loss-of-function mutations in eIF4E1 have conferred resistance in several crops (**Bastet et al., 2019**). However, its potential to influence non-VPg viral proteins remained unexplored until now. Chapter I revealed that the CRISPR/Cas9-edited in-frame deletion mutant of tomato eIF4E1 (*9DEL*) physically interacts with the CMV 2b protein. This interaction is also observed in wild-type eIF4E1. However, wild-type tomato plants remain fully susceptible to CMV infection, whereas the *9DEL* mutant exhibits partial resistance (**Atarashi et al., 2020**). This suggests that structural modifications in *eIF4E1* can alter plant-virus dynamics of resistance without abolishing protein interaction. This led to the hypothesis that the potential outcome of this interaction raises the intriguing possibility that 9DEL-eIF4E1 may inhibit 2b function and confer partial resistance, revealing a novel resistance mechanism distinct from classical recessive resistance and representing a new antiviral approach based on functional disruption of RNA silencing suppressor 2b.

This chapter investigates the impact of the 9DEL-eIF4E1 and 2b interaction on *9DEL* resistance, particularly its RNA silencing suppressor activity and influence on viral RNA accumulation based on prior evidence that 2b's silencing suppression is sensitive to subcellular localization, protein stability, and availability of RNA binding partners (**Du et al., 2014**). I also analyzed the requirement of 2b in systemic infection using CMVΔ2b mutants and quantify resistance responses in wild-type and *9DEL* tomato plants.

Results

1. **Partial inhibition of RSS activity of 2b by 9DEL-eIF4E1 interaction**

Plants employ multiple defense mechanisms to regulate host-virus interactions, including hormonal signaling pathways and protein degradation systems. CMV 2b is known to interfere with these pathways, notably salicylic acid (SA) and jasmonic acid (JA) signaling, the ubiquitin-26S proteasome system (UPS), and autophagy (**Arinaitwe et al., 2023; Crawshaw et al., 2024; Nakahara et al., 2012; Yang et al., 2020**). To determine whether 9DEL-eIF4E1 binding facilitates CMV 2b degradation via autophagy or UPS, potentially contributing to viral resistance, I co-expressed eIF4E1 and 9DEL-eIF4E1 with 2b in wild-type and *ATG7* knockout (lacking autophagy) *Nicotiana benthamiana* plants and treated with MG132- which is a 26S proteasome inhibitor. The protein levels of both eIF4E1 or 9DEL-eIF4E1 and 2b remained unchanged across NB and *ATG7ko* plants under proteasome inhibition (**Figure 4**). This suggests that neither the ubiquitin-proteasome system nor autophagy contribute significantly to the degradation of these proteins, however, the evidence remains inconclusive.

Since 2b is a key viral suppressor of RNA silencing (RSS), and 9DEL-eIF4E1 binds 2b without promoting its degradation via autophagy or the 26S-proteasome, I hypothesized that *9DEL* might instead interfere with 2b's RSS function. 2b's ability to suppress host RNA silencing is vital for CMV infection, and impaired RSS function weakens the CMV's ability to evade host defense (**Zhang et al., 2006; Lewsey et al., 2010; Wu et al., 2017**), thereby contributing to the observed resistance in *9DEL* plants (**Atarashi et al., 2020**).

To evaluate whether the interaction between 9DEL-eIF4E1 and CMV 2b has an inhibitory effect on 2b function, I examined the impact of 9DEL-eIF4E1 on the RSS activity of the 2b protein. To test this, I co-infiltrated *Nicotiana benthamiana* with GFP and 2b either alone or in combination with eIF4E1 or 9DEL-eIF4E1. As expected, co-expression of 2b with GFP resulted in robust green fluorescence, confirming the strong RSS activity of 2b (**Figure 5a**). This fluorescence was significantly reduced in leaf areas where 2b was co-expressed with 9DEL-eIF4E1 (**Figure 5a**), indicating a suppression of RSS activity of 2b. In contrast, co-expression of eIF4E1 with 2b did not produce a comparable decrease in GFP signal (**Figure 5b**), despite both eIF4E variants showing physical interaction with 2b (**Figure 1**).

Quantitative analysis of GFP fluorescence intensity using ImageJ confirmed this observation. The highest fluorescence was recorded in the co-expression of GFP with 2b, demonstrating the effect of RSS activity of 2b in the absence of 9DEL-eIF4E1 or eIF4E1 (**Figure 5b**), which significantly decreased in the presence of 9DEL-eIF4E1 (**Figure 5b**), whereas wild-type eIF4E1 had little effect (**Figure 5a, b**). However, the difference between 9DEL-eIF4E1 and eIF4E1 was not statistically different (Tukey's HSD test, $p = 0.313$), even though both protein binds to R2b. Western blot analysis further demonstrated that 2b protein levels were reduced when co-expressed with 9DEL-eIF4E1 (**Figure 5c**), suggesting that 9DEL may promote post-translational degradation of 2b. Notably, GFP mRNA levels were reduced in the presence of 9DEL-eIF4E1 (**Figure 5d**), although the reduction in mRNA levels was not statistically different compared to wild-type eIF4E1 (**Figure 5d**). Further, no significant differences were observed in the relative mRNA levels of 2b, 9DEL-eIF4E1, and eIF4E1 (**Figure 5e, f**), suggesting that the inhibitory effect of 9DEL-eIF4E1

is likely post-translational. These results suggest that 9DEL-eIF4E1 retains its established eIF4E1 function while acquiring a novel ability to suppress CMV virulence by interfering with the RSS activity of 2b. Unlike the wild-type eIF4E1 protein, in-frame *9DEL* mutant protein confers resistance through active interference with 2b viral suppressor, demonstrating a unique, gain-of-function mechanism of CMV resistance.

2. 2b is essential for CMV virulence and systemic infection in tomato

To evaluate the contribution of CMV 2b to systemic infection and to assess the impact of the 9DEL-eIF4E1 allele on systemic CMV infection, I conducted inoculation assays using *CMV-Y* (wild-type), *CMVΔ2b* (2b deletion mutant), and *CMV2bΔC* (C-terminal truncation of 2b) in both wild-type 'S8' and 9DEL tomato plants. At 35 days post-inoculation, systemic viral accumulation in non-inoculated upper leaves was quantified via DAS-ELISA. As shown in **Figure 6a**, plants inoculated with *CMVΔ2b* exhibited no CMV accumulation in both 'S8' and *9DEL* plants, confirming that the 2b protein is indispensable for efficient long-distance movement and systemic infection in tomato. In contrast, plants inoculated with *CMV-Y* or *CMV2bΔC* showed detectable systemic accumulation in both genotypes. Viral accumulation was lower in CMV-Y inoculated *9DEL* plants compared to wild-type 'S8' or susceptible tomato cultivar 'Moneymaker' (MM) plants, as indicated by reduced ELISA absorbance values (**Figure 6a, b**). These results indicate that, while CMV 2b is essential for efficient systemic infection, the 9DEL-eIF4E1 allele partially restricts viral accumulation in systemic infection consistent with previous study (**Atarashi et al., 2020)**.

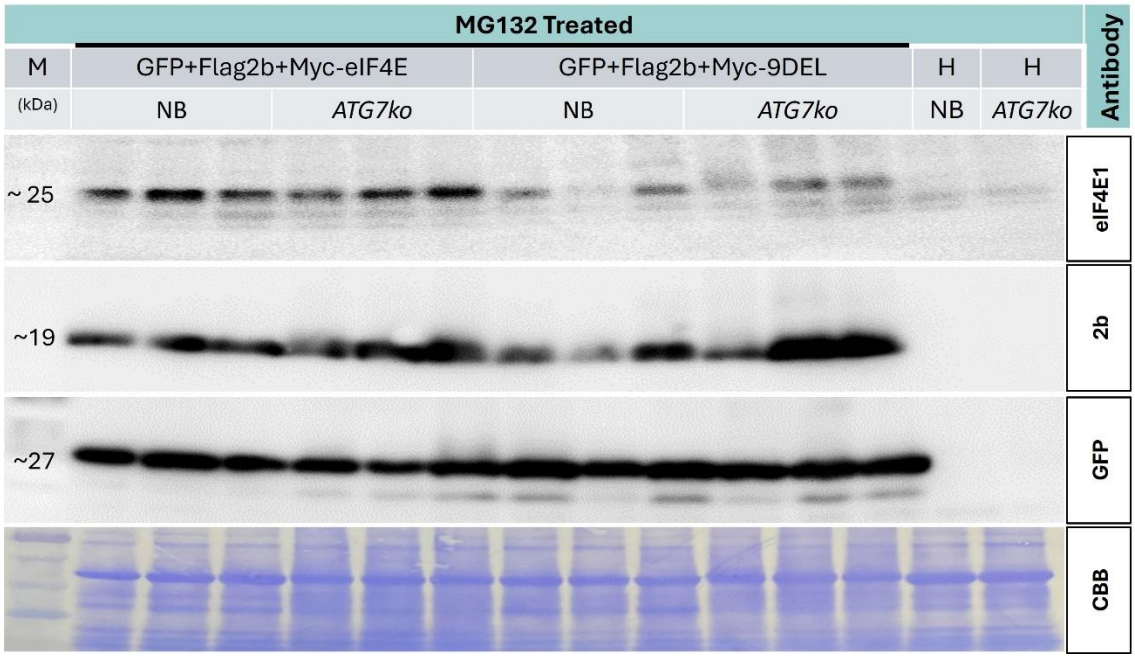

Figure 4: 9DEL-eIF4E1–mediated suppression of CMV 2b is independent of autophagy and 26S proteasomal degradation. Western blot analysis of *Nicotiana benthamiana* wild-type (NB) and autophagy-deficient ATG7 knockout (ATG7ko) leaves co-expressing GFP, Flag-2b, and Myc-eIF4E1 or Myc-9DEL, treated with 100 µM MG132 26S 26S proteasome inhibitor. Detection was performed using anti-Myc, anti-Flag, and anti-GFP antibodies. CBB staining serves as a total protein loading control. Protein levels of eIF4E1, 9DEL-eIF4E1, and 2b remained stable across all treatments, including NB and *ATG7ko* indicating that neither the proteasome nor autophagy pathways significantly contribute to their degradation. Non-infiltrated healthy (H) plants were used as negative controls to validate antibody specificity. These findings suggest that 9DEL-eIF4E1–mediated interference with 2b function does not involve proteolytic turnover but likely occurs through post-translational modulation.

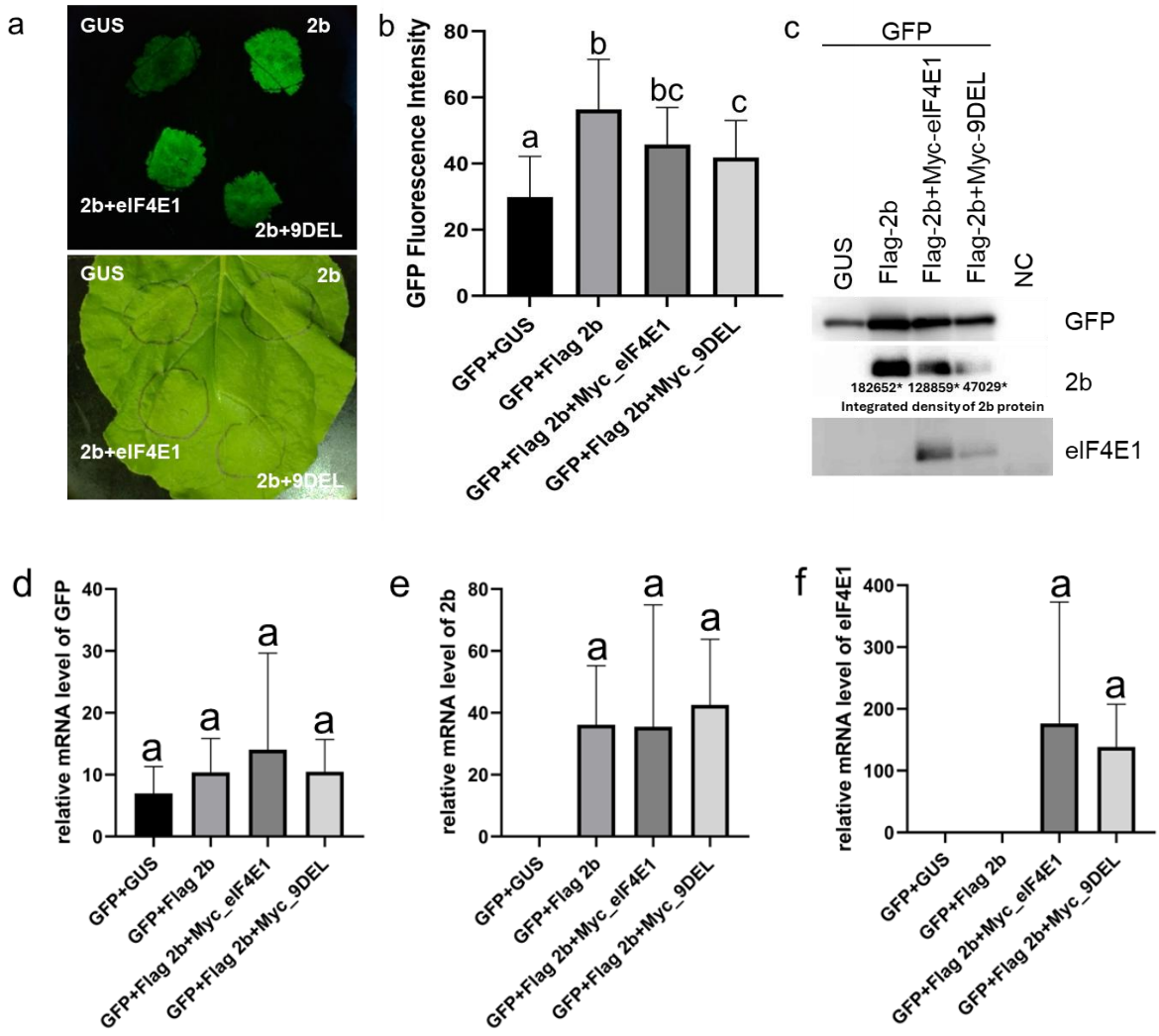

Figure 5: 9DEL partially inhibits 2b RNA silencing suppressor activity in *N. benthamiana leaves*. (a) GFP was transiently co-expressed in *N. benthamiana* leaves alongside RNA silencing suppressor Flag-tagged 2b, either alone or in combination with Myc-tagged eIF4E1 or 9DEL-eIF4E1. GUS control was included as negative control. Fluorescence image was captured under UV light at 3 days post-infiltration. (b) Quantification of GFP fluorescence intensity using ImageJ. Data represents means ± standard deviation (SD) from three independent biological replicates (n = 3). Treatments sharing the same lowercase letters are not significantly different (Tukey's HSD test, $p < 0.05$). (c) Western blot analysis

of total protein extracts using anti-GFP, anti-Flag, anti-Myc antibody to detect GFP, 2b and eIF4E1/9DEL-eIF4E1 accumulation, respectively. Integrated density of protein level was measured from three replicates using ImageJ software, values are marked with an asterisk (*). (d-f) Quantitative RT-PCR to assess mRNA levels which reflect relative transcript accumulation of GFP, 2b, and eIF4E1. Total RNA was extracted from infiltrated tissues at 3 dpi, reverse transcribed, and amplified using gene-specific primers. NBL23 was used as the internal reference gene for normalization. Relative expression values were calculated using the ΔΔCt method. Error bars represent standard deviation from three independent biological replicates (n = 3). In (b) and (d–f), the same lowercase letters indicate no significant differences in Tukey's HSD test ($p < 0.05$).

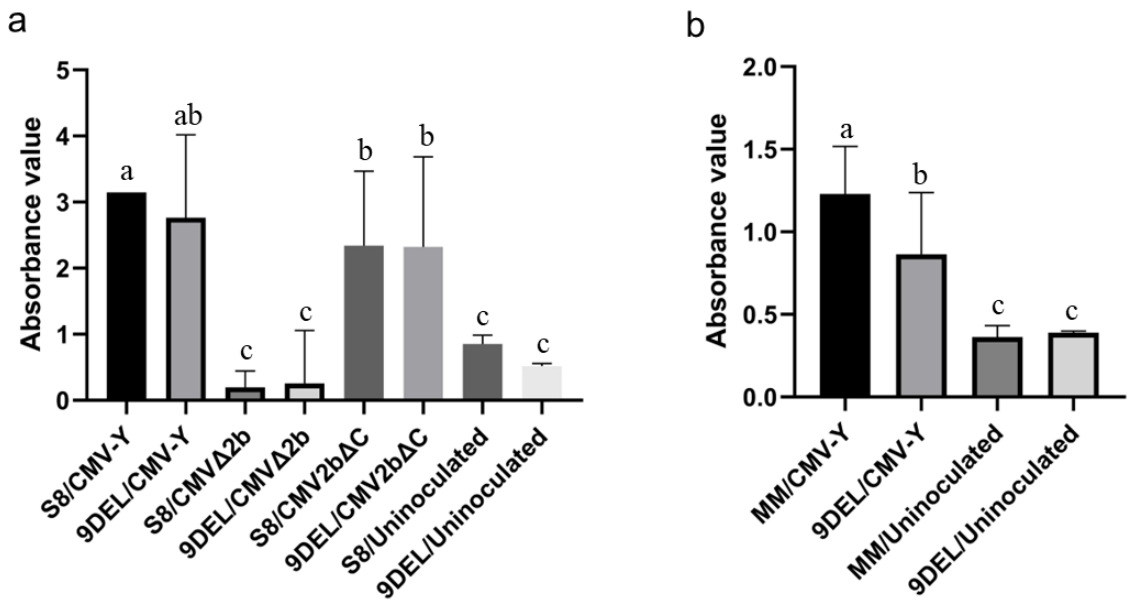

Figure 6: Inoculation tests assessing systemic CMV accumulation in tomato plants.

(a) Systemic accumulation of cucumber mosaic virus (CMV) coat protein (CP) was evaluated in uninoculated upper leaves of wild-type tomato 'S8' and *9DEL* mutant tomato plants at 35 days post-inoculation (dpi) with CMV-Y, CMVΔ2b (lacking 2b), and CMV2bΔC (C-terminal truncate of 2b). Wild-type parent 'S8' and *9DEL* mutant tomato plants were inoculated and the systemic accumulation of CMV CP in the uninoculated upper leaves was determined by ELISA at 35 days post-inoculation. (b) Parallelly, *9DEL* plant was compared with a susceptible tomato cultivar 'Money maker' in an inoculation test to assess differential virus accumulation. Viral accumulation was quantified using ELISA, and absorbance values (OD at 405 nm) are presented as mean ± standard error from at least three independent biological replicates ($n > 3$). One-way ANOVA followed by Tukey's HSD test was performed to analyze the significant differences among the multiple treatment groups indicated by lowercase letters between groups ($p < 0.05$).

Discussion

The 2b protein of cucumber mosaic virus (CMV) is a multifunctional virulence factor essential for suppressing host RNA silencing and enabling systemic infection (**Zhang et al., 2006; Lewsey et al., 2010; Du et al., 2014**). The observed interaction between 9DEL-eIF4E1 and CMV 2b in this study is likely a key factor contributing to CMV resistance in *9DEL* plants. To explore this further, I evaluated whether the genome-edited 9DEL-eIF4E1 interferes with the 2b function, contributing to enhanced CMV resistance.

The findings demonstrate that, while both wild-type eIF4E1 and 9DEL-eIF4E1 interact with 2b (**Figure 1**), but only the 9DEL variant attenuated its RSS activity, as evidenced by reduced GFP fluorescence and protein levels when co-expressed with 2b (**Figure 4b, c**). Although the differences were not statistically significant, the consistent suppression of 2b protein accumulation and GFP expression in the presence of 9DEL-eIF4E1 (**Figure 4 b, c**), indicating partial suppression of RSS activity of 2b. In contrast, wild-type eIF4E1 had a minimal effect on 2b RSS activity (**Figure 4b**). Quantitative analysis confirmed that fluorescence intensity was significantly reduced in the *9DEL* combination compared to 2b alone (**Figure 4b**), although the reduction was not statistically different from the wild-type eIF4E1 combination (Tukey's HSD, $p = 0.313$). Such suppression could diminish the ability of 2b to accumulate siRNAs and inhibit AGO1, partially restoring the host's antiviral RNAi defense (**Zhang et al., 2006; Lewsey et al., 2010**). Western blot analysis further revealed that 2b protein levels were lower in the presence of 9DEL-eIF4E1 (**Figure 4c**), suggesting possible post-translational degradation or destabilization of 2b. While mRNA levels of GFP, 2b, and eIF4E1 showed no significant changes across treatments

(**Figures 4d–f**), the reduction of GFP and 2b protein implies that 9DEL-eIF4E1 acts post-translationally to suppress 2b activity and viral protein accumulation. This aligns with earlier findings indicating that 2b stability and function can be influenced by host factors (**Nakahara et al., 2012; Shukla et al., 2022**).

To assess whether this interference affected CMV systemic infection, I inoculated wild-type 'S8' and *9DEL* tomato plants with *CMV-Y*, *CMVΔ2b* (mutant lacking 2b), and *CMV2bΔC* (C-terminally truncated 2b mutant). As expected, *CMVΔ2b* failed to accumulate systemically in both plant genotypes (**Figure 5a**), confirming the essential role of 2b in systemic infection (**Lewsey et al., 2009; Zhou et al., 2014; Khaing et al., 2020b**). However, 9DEL plants inoculated with *CMV-Y* or *CMV2bΔC* showed reduced viral accumulation compared to wild-type 'S8' plants, suggesting that 9DEL-eIF4E1 impairs, but does not completely inhibit, 2b-dependent CMV infection. Further, when compared with a susceptible tomato cultivar 'Moneymaker,' *9DEL* plants showed significantly lower CMV accumulation (**Figure 5b**), further supporting a protective role of 9DEL-eIF4E1 against CMV.

These findings suggest that 9DEL-eIF4E1 contributes to partial CMV resistance by inhibiting 2b's RSS function and possibly other virulence-associated activities. Beyond silencing suppression, 2b is known to interfere with hormonal defense signaling (**Wu et al., 2017; Ji et al., 2021**) and autophagy-related antiviral responses (**Jeon et al., 2017; Shukla et al., 2022**), which may also be indirectly affected by *9DEL* binding. The results support a model in which the 9DEL-eIF4E1 protein, though structurally competent for 2b binding, interferes with its functions essential for CMV infection. Such mechanisms have been observed in artificial resistance alleles of eIF4E conferring broad resistance to

potyviruses (**Charron et al., 2008; Piron et al., 2010; Bastet et al., 2018**). This supports a novel antiviral mechanism distinct from classical recessive resistance and highlights the potential of in-frame genome editing as a targeted strategy for developing viral resistance in crops.

GENERAL DISCUSSION

Developing sustainable viral resistant crops remains a key objective in modern plant biotechnology. Among the resistance mechanisms explored, the modification of host susceptibility genes, particularly eIF4E and its isoforms, has emerged as a central strategy. Natural mutations in eIF4E and translation-related factors account for nearly half of all known virus resistance sources in plants (**Zlobin and Taranov, 2023**), typically functioning through loss-of-function alleles that prevent viral exploitation of host machinery. In CMV, a well-documented example includes the eIF4E mutant in Arabidopsis, which confers resistance by preventing the virus from interacting with the host factor (**Yoshii et al., 2004; Zhou et al., 2014; Gao et al., 2018; Zhao et al., 2018; Shukla et al., 2022; Yoon et al., 2020; Yu et al., 2020**). However, in a previous study by **Atarashi et al. (2020**), the 9DEL-eIF4E1 allele, created via CRISPR/Cas-editing, contains a precise 9-nucleotide in-frame deletion that translates protein from the entire open reading frame of eIF4E1 confers CMV resistance through a gain-of-function mechanism. The *1INS* frameshift mutant that seems to be a complete loss of eIF4E1 function, does not affect the susceptibility to CMV (**Atarashi et al., 2020**). 9DEL-eIF4E1 appears to confer resistance arise from 9DEL-eIF4E1's ability to interfere with the activity of CMV 2b, a key viral suppressor of RNA silencing.

The findings demonstrated that 9DEL-eIF4E1 binds to CMV 2b, with interaction affinity comparable to wild-type eIF4E1, as confirmed through yeast two-hybrid and split-luciferase assays (**Figure 1 & 2**). However, only 9DEL-eIF4E1 was associated with a reduction in 2b function, as indicated by decreased RNA silencing suppressor (RSS) activity **(Figure 5)** and lower systemic CMV accumulation in tomato **(Figure 6)**. These

results support the notion that resistance arises not from altered binding capacity but from downstream functional interference, potentially via conformational modification or disruption of 2b's ability to interfere with the host silencing mechanism. A proposed model of this resistance mechanism is illustrated in **Figure 7**, showing the importance of 2b in systemic infection of CMV in tomato, and the disruption of 2b's activity by 9DEL-eIF4E1, resulting in partial resistance.

This interpretation aligns with the broader functional complexity of CMV 2b, which acts not only as an RSS protein but also as a suppressor of salicylic acid and jasmonic acid hormonal signaling and an antagonist of autophagy-related antiviral responses (**Lewsey et al., 2009; Wu et al., 2017; Ji et al., 2021; Arinaitwe et al., 2023; Crawshaw et al., 2024; Zhang et al., 2024; Jeon et al., 2017; Shukla et al., 2022; Tong et al., 2023; Nakahara et al., 2012; Yang et al., 2020**). Therefore, the *9DEL* mutation may disrupt not only RNAi suppression but also multiple 2b-mediated host manipulations. Notably, this study contributes to the expanding evidence that in-frame modifications can produce alleles with superior and novel resistance properties. For example, specific amino acid changes in eIF4E have been shown to confer broader potyvirus resistance than complete knockouts (**Charron et al., 2008; Piron et al., 2010; Poulicard et al., 2016; Nekrasov et al., 2017; Bastet et al., 2018**). A similar trend has been observed for powdery mildew resistance in *MLO* genes (**Nekrasov et al., 2017**). strategic advancement, shifting from traditional loss-of-function approaches to the functional editing of host factors that antagonize viral effector activity.

In conclusion, 9DEL-eIF4E1 defines a novel resistance mechanism in which a structurally functional host protein inhibits a viral suppressor through editing, mutation-specific effect.

This finding not only clarifies the molecular basis of CMV resistance in *9DEL* tomato but also highlights the potential of precise gain-of-function alleles as a targeted strategy for developing durable antiviral resistance.

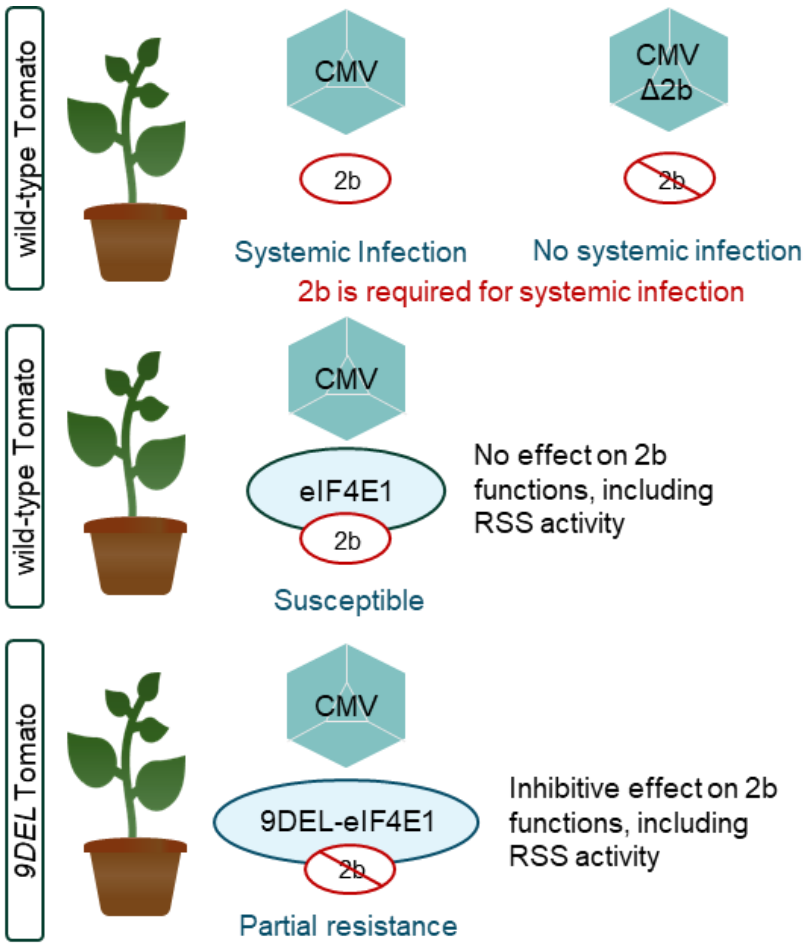

Figure 7: Proposed mechanism of *9DEL*-mediated CMV resistance. The diagram illustrates a potential mechanism for CMV resistance in CRISPR/Cas9-edited 9DEL tomato plants. CMVΔ2b (lacking 2b) fails to establish systemic infection, highlighting the essential role of 2b in CMV systemic infection in tomato plants. CMV requires its 2b protein to suppress host RNA silencing and enable systemic infection. In wild-type plants, 2b interacts with eIF4E1 to promote viral spread, resulting in susceptibility. In *9DEL* plants, although 2b still binds to the mutant 9DEL-eIF4E1, this interaction inhibits 2b's RNA silencing suppressor activity, reducing viral systemic infection and leading to partial resistance.

SUMMARY

Plant viruses, such as the cucumber mosaic virus (CMV) pose major threats to global agriculture by infecting a wide range of economically important crops, including tomato. CMV 2b is a multifunctional protein known to suppress host RNA silencing, interferes with plant defense pathways, and enhances viral virulence. Eukaryotic translation initiation factor 4E1 (eIF4E1) is a known susceptibility factor commonly interfering with VPg proteins of potyviruses, and its mutations have been widely associated with virus resistance in crops.

This study investigated the molecular basis of CMV resistance in a genome-edited tomato line (*9DEL*) harboring a 9-nucleotide in-frame deletion in eIF4E1. Initial protein-protein interaction assays using yeast two-hybrid demonstrated that both wild-type eIF4E1 and 9DEL-eIF4E1 interact with CMV 2b, but not with other viral proteins such as coat or movement proteins. Yeast two-hybrid and split-luciferase complementation assays confirmed this interaction, and subcellular co-localization revealed overlapping signals between 2b and both eIF4E1 variants in the cytoplasm and nucleus. This is the first report demonstrating the eIF4E1 and CMV 2b interaction.

Despite similar binding affinity, only 9DEL-eIF4E1 attenuated the RNA silencing suppressor (RSS) activity of 2b in GFP co-expression assays. In these assays, co-expression of 2b with 9DEL-eIF4E1 led to a noticeable reduction in GFP fluorescence compared to co-expression with wild-type eIF4E1, indicating that 9DEL-eIF4E1 interferes with 2b's ability to suppress RNA silencing. Western blot analysis further confirmed that 2b protein levels were lower when co-expressed with 9DEL-eIF4E1, suggesting that 9DEL-eIF4E1 may destabilize 2b at the post-translational level. Importantly, qRT-PCR showed no

significant differences in the mRNA levels of GFP, 2b, or eIF4E1 between treatments, thereby excluding transcriptional effects and supporting a model in which 9DEL-eIF4E1 post-translationally impairs 2b function, ultimately reducing its RSS activity.

Inoculation experiments further validated the functional significance of this interaction. CMV lacking 2b failed to establish systemic infection in both wild-type and *9DEL* plants, underscoring the essentiality of 2b in CMV virulence in tomato. Importantly, CMV-Y and its C-terminal truncated 2b mutant accumulated less efficiently in *9DEL* plants compared to wild-type or susceptible controls, suggesting that *9DEL* confers partial resistance by impairing 2b-dependent systemic infection.

Collectively, this study provides the first evidence that eIF4E1 physically interacts with CMV 2b and that 9DEL-eIF4E1 mutant allele attenuates 2b function. This resistance mechanism does not rely on complete loss of susceptibility, but a gain-of-function that interferes with viral RSS activity. The findings expand the antiviral role of eIF4E1 beyond its known interaction with VPg and propose a novel resistance strategy, precise in-frame genome editing of host factors to target viral suppressors, offering a promising direction for sustainable resistance breeding.

REFERENCES

Akhter, Md.S., Nakahara, K.S., Masuta, C. (2021). Resistance induction based on the understanding of molecular interactions between plant viruses and host plants. *Virol J* 18: 176.

Arinaitwe, W., Tungadi, T.D., Pate, A.E., Joyce, J., Baek, E., Murphy, A.M., Carr, J.P. (2023). Induction of aphid resistance in tobacco by the cucumber mosaic virus CMVΔ2b mutant is jasmonate-dependent. *Mol Plant Pathol* 24: 391–395.

Atarashi, H., Jayasinghe, W.H., Kwon, J., Kim, H., Taninaka, Y., Igarashi, M., Ito, K., Yamada, T., Masuta, C., Nakahara, K.S. (2020). Artificially Edited Alleles of the Eukaryotic Translation Initiation Factor 4E1 Gene Differentially Reduce Susceptibility to Cucumber Mosaic Virus and Potato Virus Y in Tomato. *Front Microbiol* 11: 564310.

Bastet, A., Lederer, B., Giovinazzo, N., Arnoux, X., German-Retana, S., Reinbold, C., Brault, V., Garcia, D., Djennane, S., Gersch, S., Lemaire, O., Robaglia, C., Gallois, J.L. (2018). Trans-species synthetic gene design allows resistance pyramiding and broad-spectrum engineering of virus resistance in plants. *Plant Biotechnol J* 16: 1569–1581.

Bastet, A., Robaglia, C., Gallois, J.L. (2017). eIF4E Resistance: Natural Variation Should Guide Gene Editing. *Trends Plant Sci* 22: 411-419.

Bastet, A., Zafirov, D., Giovinazzo, N., Guyon-Debast, A., Nogué, F., Robaglia, C., Gallois, J.L. (2019). Mimicking natural polymorphism in eIF4E by CRISPR-Cas9 base editing is associated with resistance to potyviruses. *Plant Biotechnol J* 17: 1736–1750.

Caranta, C., Pflieger, S., Lefebvre, V., Daubèze, A.M., Thabuis, A., Palloix, A. (2002). QTLs involved in the restriction of cucumber mosaic virus (CMV) long-distance movement in pepper. *Theor Appl Genet* 104: 586–591.

Chandrasekaran, J., Brumin, M., Wolf, D., Leibman, D., Klap, C., Pearlsman, M., Sherman, A., Arazi, T., Gal-On, A. (2016). Development of broad virus resistance in non-transgenic cucumber using CRISPR/Cas9 technology. *Mol Plant Pathol* 17:1140–1153.

Charron, C., Nicolaï, M., Gallois, J.L., Robaglia, C., Moury, B., Palloix, A., Caranta, C. (2008). Natural variation and functional analyses provide evidence for co-evolution between plant eIF4E and potyviral VPg. *Plant J* 54: 56–68.

Chen, H., Zou, Y., Shang, Y., Lin, H., Wang, Y., Cai, R., Tang, X., Zhou, J.M. (2008a). Firefly luciferase complementation imaging assay for protein-protein interactions in plants. *Plant Physiol* 146: 368–376.

Chen, H.Y., Yang, J., Lin, C., Yuan, Y.A. (2008b). Structural basis for RNA-silencing suppression by Tomato aspermy virus protein 2b. *EMBO Rep* 9: 754–760.

Crawshaw, S., Murphy, A.M., Rowling, P.J.E., Nietlispach, D., Itzhaki, L.S., Carr, J.P. (2024). Investigating the Interactions of the Cucumber Mosaic Virus 2b Protein with the Viral 1a Replicase Component and the Cellular RNA Silencing Factor Argonaute 1. *Viruses* 16: 676.

Du, Z., Chen, A., Chen, W., Liao, Q., Zhang, H., Bao, Y., Roossinck, M.J., Carr, J.P. (2014). Nuclear-cytoplasmic partitioning of cucumber mosaic virus protein 2b determines the balance between its roles as a virulence determinant and an RNA-silencing suppressor. *J Virol* 88: 5228-41.

Gao, L., Luo, J., Ding, X., Wang, T., Hu, T., Song, P., Zhai, R., Zhang, H., Zhang, K., Li, K., Zhi, H. (2020). Soybean RNA interference lines silenced for eIF4E show broad potyvirus resistance. *Mol Plant Pathol* 21: 303–317.

Gao, S., Lu, J., Cheng, X., Gu, Z., Liao, Q., Du, Z. (2018). Heterologous replicase from cucumoviruses can replicate viral RNAs, but is defective in transcribing subgenomic RNA4a or facilitating viral movement. *Viruses* 10: 590.

Gao, Y., Yang, J., Zhang, X., Chen, A., Gu, Z., Du, Z. (2021). The Weak Small RNA-Binding Activity of the 2b Proteins of Subgroup II Cucumber Mosaic Virus Strains Is Insufficient for RNA Silencing Suppression. *Front Microbiol* 12: 760937.

Garcia-Ruiz, H. (2018). Susceptibility Genes to Plant Viruses. *Viruses* 10: 484.

Gauffier, C., Lebaron, C., Moretti, A., Constant, C., Moquet, F., Bonnet, G., Caranta, C., Gallois, J.L. (2016). A TILLING approach to generate broad-spectrum resistance to potyviruses in tomato is hampered by eIF4E gene redundancy. *Plant J* 85: 717–729.

Ghoshal, B., and Sanfaçon, H. (2015). Symptom recovery in virus-infected plants: Revisiting the role of RNA silencing mechanisms. *Virology* 479-480: 167-79.

González, I., Martínez, L., Rakitina, D.V., Lewsey, M.G., Atencio, F.A., Llave, C., Kalinina, N.O., Carr, J.P., Palukaitis, P., Canto, T. (2010). Cucumber Mosaic Virus 2b Protein Subcellular Targets and Interactions: Their Significance to RNA Silencing Suppressor Activity. *Mol Plant Microbe Interact* 23: 294–303.

González, I., Martínez, L., Rakitina, D.V., Lewsey, M.G., Atencio, F.A., Llave, C., Kalinina, N.O., Carr, J.P., Palukaitis, P., Canto, T. (2010). Cucumber mosaic virus 2b protein subcellular targets and interactions: their significance to RNA silencing suppressor activity. *Mol Plant Microbe Interact* 23: 294-303.

Goto, K., Kobori, T., Kosaka, Y., Natsuaki, T., Masuta, C. (2007). Characterization of Silencing Suppressor 2b of Cucumber Mosaic Virus Based on Examination of its Small RNA-Binding Abilities. *Plant Cell Physiol* 48: 1050–1060.

Hirsch, J., and Moury, B. (2021). Cucumber Mosaic Virus (Bromoviridae). *Encyclopedia of Virology. Elsevier,* pp. 371–382.

Horstman, A., Tonaco, I., Boutilier, K., Immink, R. (2014). A Cautionary Note on the Use of Split-YFP/BiFC in Plant Protein-Protein Interaction Studies. *Int J Mol Sci* 15:9628–9643.

Huang, J., Du, J., Liu, Y., Lu, L., Xu, Y., Shi, J., Liu, Q., Li, Q., Liu, Y., Chen, Y., Du, M., Zhao, Y., Huo, L., Wang, W., Ding, C., Wei, L., Wu, J., Yuan, Y.W., Chen, J., Li, R. (2025). RH3 enhances antiviral defense by facilitating small RNA loading into Argonaute 2 at endoplasmic reticulum–chloroplast membrane contact sites. *Nat Commun* 16: 1953.

Jeon, E.J., Tadamura, K., Murakami, T., Inaba, J-I., Kim, B.M., Sato, M., Atsumi, G., Kuchitsu, K., Masuta, C., Nakahara, K.S. (2017). rgs-CaM Detects and Counteracts Viral RNA Silencing Suppressors in Plant Immune Priming. *J Virol* 91: e00761-17.

Ji, M., Zhao, J., Han, K., Cui, W., Wu, X., Chen, B., Lu, Y., Peng, J., Zheng, H., Rao, S., Wu, G., Chen, J., Yan, F. (2021). Turnip mosaic virus P1 suppresses JA biosynthesis by degrading

cpSRP54 that delivers AOCs onto the thylakoid membrane to facilitate viral infection. *PLoS Pathog* 17: e1010108.

Kataoka, J., Masuta, C., Takanami, Y. (1990). Complete nucleotide sequence of RNA1 of cucumber mosaic virus Y strain and evolutionary relationships among genome RNAs of the virus strains. *Jpn J Phytopathol* 56: 501–507.

Khaing, Y.Y., Kobayashi, Y., Takeshita, M. (2020a). The C-terminal region of the 2a protein and 2b protein of cucumber mosaic virus are involved in the induction of shoestring-like leaf blade in tomato. *Virus Res* 289: 198172.

Khaing, Y.Y., Kobayashi, Y., Takeshita, M. (2020b). The 2b protein and C-terminal region of the 2a protein indispensably facilitate systemic movement of cucumber mosaic virus in radish with supplementary function by either the 3a or the coat protein. *Virol J* 17: 49.

Kim, H., Shimura, H., Sueda, K., Masuta, C. (2022). Importin/Exportin-mediated nucleocytoplasmic shuttling of cucumber mosaic virus 2b protein is required for 2b's efficient suppression of RNA silencing. *PLoS Pathog* 18: e1010267.

Kuroiwa, K., Danilo, B., Perrot, L., Thenault, C., Veillet, F., Delacote, F., Duchateau, P., Nogué, F., Mazier, M., Gallois, J.L. (2023). An iterative gene-editing strategy broadens eIF4E1 genetic diversity in Solanum lycopersicum and generates resistance to multiple potyvirus isolates. *Plant Biotechnol J* 21: 918–930.

Kuroiwa, K., Thenault, C., Nogué, F., Perrot, L., Mazier, M., Gallois, J.L. (2022). CRISPR-based knock-out of eIF4E2 in a cherry tomato background successfully recapitulates resistance to pepper veinal mottle virus. *Plant Sci* 316: 111160.

Lewsey, M., Surette, M., Robertson, F.C., Ziebell, H., Choi, S.H., Ryu, K.H., Canto, T., Palukaitis, P., Payne, T., Walsh, J.A., Carr, J.P. (2009). The Role of the Cucumber mosaic virus 2b Protein in Viral Movement and Symptom Induction. *Mol Plant Microbe Interact* 22: 642–654.

Lewsey, M.G., Murphy, A.M., MacLean, D., Dalchau, N., Westwood, J.H., Macaulay, K., Bennett, M.K., Moulin, M., Hanke, D.E., Powell, G., Smith, A.G., Carr, J.P. (2010). Disruption of two defensive signaling pathways by a viral RNA silencing suppressor. *Mol Plant Microbe Interact* 23: 835-45.

Li, N., Yu, C., Yin, Y., Gao, S., Wang, F., Jiao, C., Yao, M. (2020). Pepper Crop Improvement Against Cucumber Mosaic Virus (CMV): A Review. *Front Plant Sci* 11: 598798.

Liu, S., Chen, M., Li, R., Li, W.X., Gal-On, A., Jia, Z., Ding, S.W. (2022). Identification of positive and negative regulators of antiviral RNA interference in Arabidopsis thaliana. *Nat Commun* 13: 2994.

Masuta, C., Inaba, J., Shimura, H. (2012). The 2b proteins of Cucumber mosaic virus generally have the potential to differentially induce necrosis on Arabidopsis. *Plant Signal Behav* 7: 43–45.

Matsuo, K., Hong, J.S., Tabayashi, N., Ito, A., Masuta, C., Matsumura, T. (2007). Development of Cucumber mosaic virus as a vector modifiable for different host species to produce therapeutic proteins. *Planta* 225: 277–286.

Mazier, M., Flamain, F., Nicolaï, M., Sarnette, V., Caranta, C. (2011). Knock-down of both eIF4E1 and eIF4E2 genes confers broad-spectrum resistance against potyviruses in tomato. *PLoS One* 6: e29595.

Mehla, J., Caufield, J.H., Uetz, P. (2015). Mapping protein-protein interactions using yeast two-hybrid assays. *Cold Spring Harb Protoc* 2015: 442–452.

Moury, B., Lebaron, C., Szadkowski, M., Ben Khalifa, M., Girardot, G., Bolou Bi, B.A., Koné, D., Nitiema, L.W., Fakhfakh, H., Gallois, J.L. (2020). Knock-out mutation of eukaryotic initiation factor 4E2 (eIF4E2) confers resistance to pepper veinal mottle virus in tomato. *Virology* 539: 11–17.

Murota, K., Shimura, H., Takeshita, M., Masuta, C. (2017). Interaction between Cucumber mosaic virus 2b protein and plant catalase induces a specific necrosis in association with proteasome activity. *Plant Cell Rep* 36: 37–47.

Nakahara, K.S., Masuta, C., Yamada, S., Shimura, H., Kashihara, Y., Wada, T.S., Meguro, A., Goto, K., Tadamura, K., Sueda, K., Sekiguchi, T., Shao, J., Itchoda, N., Matsumura, T., Igarashi, M., Ito, K., Carthew, R.W., Uyeda, I. (2012). Tobacco calmodulin-like protein provides secondary defense by binding to and directing degradation of virus RNA silencing suppressors. *Proc Natl Acad Sci U S A* 109: 10113–10118.

Nekrasov, V., Wang, C., Win, J., Lanz, C., Weigel, D., Kamoun, S. (2017). Rapid generation of a transgene-free powdery mildew resistant tomato by genome deletion. *Sci Rep* 7: 482.

Nicaise, V., German-Retana, S., Sanjuán, R., Dubrana, M.P., Mazier, M., Maisonneuve, B., Candresse, T., Caranta, C., Le, Gall-O. (2003). The eukaryotic translation initiation factor

4E controls lettuce susceptibility to the Potyvirus Lettuce mosaic virus. *Plant Physiol* 132:1272–1282.

Otagaki, S., Arai, M., Takahashi, A., Goto, K., Hong, J.S., Masuta, C., Kanazawa, A. (2006). Rapid induction of transcriptional and post-transcriptional gene silencing using a novel Cucumber mosaic virus vector. *Plant Biotechnol* 23: 259–265.

Pagán, I. (2019). CHAPTER 16: Movement Between Plants: Vertical Transmission. Cucumber Mosaic Virus. *The American Phytopathological Society*, pp. 185–198.

Palukaitis, P. (2019). CHAPTER 10: Genome Structure and Expression. Cucumber Mosaic Virus. *The American Phytopathological Society*, pp. 113–121.

Palukaitis, P., Roossinck, M.J., Dietzgen, R.G., Francki, R.I.B. (1992). Cucumber MOSAIC Virus. *Adv Virus Res* 41: 281–348.

Piron, F., Nicolaï, M., Minoïa, S., Piednoir, E., Moretti, A., Salgues, A., Zamir, D., Caranta, C., Bendahmane, A. (2010). An induced mutation in tomato eiF4E leads to immunity to two potyviruses. *PLoS One* 5: e11313.

Poulicard, N., Pacios, L.F., Gallois, J.L., Piñero, D., García-Arenal, F. (2016). Human Management of a Wild Plant Modulates the Evolutionary Dynamics of a Gene Determining Recessive Resistance to Virus Infection. *PLoS Genet* 12: e1006214.

Ruffel, S., Dussault, M.H., Palloix, A., Moury, B., Bendahmane, A., Robaglia, C., Caranta, C. (2002). A natural recessive resistance gene against potato virus Y in pepper corresponds to the eukaryotic initiation factor 4E (eIF4E). *Plant J* 32:1067–1075.

Ryabov, E.V., Fraser, G., Mayo, M.A., Barker, H., Taliansky, M. (2001). Umbravirus Gene Expression Helps Potato leafroll virus to Invade Mesophyll Tissues and to be Transmitted Mechanically between Plants. *Virology* 286: 363–372.

Scholthof, K.B.G., Adkins, S., Czosnek, H., Palukaitis, P., Jacquot, E., Hohn, T., Hohn, B., Saunders, K., Candresse, T., Ahlquist, P., Hemenway, C., Foster, G.D. (2011). Top 10 plant viruses in molecular plant pathology. *Mol Plant Pathol* 12: 938–954.

Shan, H., Chen, D., Zhang, R., Wang, X., Li, J., Wang, C., Li, Y., Huang, Y. (2023). Relationship between Sugarcane eIF4E Gene and Resistance against Sugarcane Streak Mosaic Virus. *Plants* 12: 2805.

Shi, B.J., Palukaitis, P. (2011). The N-terminal 12 amino acids of tomato aspermy virus 2b protein function in infection and recombination. *J Gen Virol* 92: 2706–2710.

Shukla, A., Hoffmann, G., Kushwaha, N.K., López-González, S., Hofius, D., Hafrén, A. (2022). Salicylic acid and the viral virulence factor 2b regulate the divergent roles of autophagy during cucumber mosaic virus infection. *Autophagy* 18: 1450–1462.

Sueda, K., Shimura, H., Meguro, A., Uchida, T., Inaba, J., Masuta, C. (2010). The C-terminal residues of the 2b protein of Cucumber mosaic virus are important for efficient expression in Escherichia coli and DNA-binding. *FEBS Lett* 584: 945–950.

Sunpapao, A., Nakai, T., Dong, F., Mochizuki, T., Ohki, S.T. (2009). The 2b protein of cucumber mosaic virus is essential for viral infection of the shoot apical meristem and for efficient invasion of leaf primordia in infected tobacco plants. *J Gen Virol* 90: 3015–3021.

Suzuki, M., Kuwata, S., Kataoka, J., Masuta, C., Nitta, N., Takanami, Y. (1991). Functional analysis of deletion mutants of cucumber mosaic virus RNA3 using an in vitro transcription system. *Virology* 183: 106–113.

Takahashi, H., Tabara, M., Miyashita, S., Ando, S., Kawano, S., Kanayama, Y., Fukuhara, T., Kormelink, R. (2022). Cucumber Mosaic Virus Infection in Arabidopsis: A Conditional Mutualistic Symbiont? *Front Microbiol* 12: 770925.

Tatineni, S., and Hein, G.L. (2023). Plant Viruses of Agricultural Importance: Current and Future Perspectives of Virus Disease Management Strategies. *Phytopathology* 113: 117–141.

Tong, X., Zhao, J.J., Feng, Y.L., Zou, J.Z., Ye, J., Liu, J., Han, C., Li, D., Wang, X.B. (2023). A selective autophagy receptor VISP1 induces symptom recovery by targeting viral silencing suppressors. *Nat Commun* 14: 3852.

Tungadi, T., Groen, S.C., Murphy, A.M., Pate, A.E., Iqbal, J., Bruce, T.J.A., Cunniffe, N.J., Carr, J.P. (2017). Cucumber mosaic virus and its 2b protein alter emission of host volatile organic compounds but not aphid vector settling in tobacco. *Virol J* 14: 91.

Wang, R., Du, Z., Bai, Z., Liang, Z. (2017). The interaction between endogenous 30S ribosomal subunit protein S11 and Cucumber mosaic virus LS2b protein affects viral replication, infection and gene silencing suppressor activity. *PLoS One* 12: e0182459.

Wu, D., Qi, T., Li, W.X., Tian, H., Gao, H., Wang, J., Ge, J., Yao, R., Ren, C., Wang, X.B., Liu, Y., Kang, L., Ding, S.W., Xie, D. (2017). Viral effector protein manipulates host hormone signaling to attract insect vectors. *Cell Res* 27: 402–415.

Yang, M., Ismayil, A., Liu, Y. (2020). Autophagy in Plant-Virus Interactions. *Annu Rev Virol* 7: 403–419.

Yoon, Y.J., Venkatesh, J., Lee, J.H., Kim, J., Lee, H.E., Kim, D.S., Kang, B.C. (2020). Genome Editing of eIF4E1 in Tomato Confers Resistance to Pepper Mottle Virus. *Front Plant Sci* 11: 1098.

Yoshii, M., Nishikiori, M., Tomita, K., Yoshioka, N., Kozuka, R., Naito, S., Ishikawa, M. (2004). The Arabidopsis Cucumovirus Multiplication 1 and 2 Loci Encode Translation Initiation Factors 4E and 4G. *J Virol* 78: 6102–6111.

Yu, D., Liao, L., Zhang, J., Zhang, Y., Xu, K., Liu, K., Li, X., Tan, G., Chen, R., Wang, Y., Liu, X., Zhang, X., Han, X., Wei, Z., Li, C. (2020). A novel, easy and rapid method for constructing yeast twohybrid vectors using In-Fusion technology. *Biotechniques* 64: 219–224.

Zhang, J.R., Liu, Y.M., Li, D., Wu, Y.J., Zhao, S.X., Wang, X.W., Liu, S.S., Walling, L.L., Pan, L.L. (2024). Viral proteins resolve the virus-vector conundrum during hemipteran-mediated transmission by subverting salicylic acid signaling pathway. *Nat Commun* 15: 9448.

Zhang, X., Li, H., Zhang, J., Zhang, C., Gong, P., Ziaf, K., Xiao, F., Ye, Z. (2011). Expression of artificial microRNAs in tomato confers efficient and stable virus resistance in a cell-autonomous manner. *Transgenic Res* 20: 569-81.

Zhang, X., Yuan, Y.R., Pei, Y., Lin, S.S., Tuschl, T., Patel, D.J., Chua, N.H. (2006). Cucumber mosaic virus -encoded 2b suppressor inhibits Arabidopsis Argonaute1 cleavage activity to counter plant defense. *Genes Dev* 20: 3255–3268.

Zhao, J.H., Liu, X.L., Fang, Y.Y., Fang, R.X., Guo, H.S. (2018). CMV2b-Dependent regulation of host defense pathways in the context of viral infection. *Viruses* 10: 618.

Zhao, Z., Yang, S.J., Yin, X.X., Yan, X.L., Hassan, B., Fan, J., Li, Y., Wang, W. (2023). ARGONAUTE 1: a node coordinating plant disease resistance with growth and development. *Phytopathol Res* 5: 38.

Zhou, L.X., Tian, Y.P., Ren, L.L., Yan, Z.Y., Jiang, J., Shi, Q.H., Geng, C., Li, X.D. (2024). A natural substitution of a conserved amino acid in eIF4E confers resistance against multiple potyviruses. *Mol Plant Pathol* 25: e13418.

Zhou, T., Murphy, A.M., Lewsey, M.G., Westwood, J.H., Zhang, H.M., González, I., Canto, T., Carr, J.P. (2014). Domains of the cucumber mosaic virus 2b silencing suppressor protein affecting inhibition of salicylic acid-induced resistance and priming of salicylic acid accumulation during infection. *J Gen Virol* 95: 1408–1413.

Zhou, Z., Bi, G., Zhou, J.M. (2018). Luciferase Complementation Assay for Protein-Protein Interactions in Plants. *Curr Protoc Plant Biol* 3: 42–50.

Ziebell, H., Murphy, A.M., Groen, S.C., Tungadi, T., Westwood, J.H., Lewsey, M.G., Moulin, M., Kleczkowski, A., Smith, A.G., Stevens, M., Powell, G., Carr, J.P. (2011). Cucumber mosaic virus and its 2b RNA silencing suppressor modify plant-aphid interactions in tobacco. *Sci Rep* 1: 187

Zitter, T.A., and Murphy, J.F. (2009). Cucumber Mosaic. *Plant Health Instr* 9.

Zlobin, N., and Taranov, V. (2023). Plant eIF4E isoforms as factors of susceptibility and resistance to potyviruses. *Front Plant Sci* 14: 1041868.

ACKNOWLEDGMENTS

I am deeply grateful to have completed my doctoral course at the Graduate School of Agriculture, Hokkaido University. The path to this thesis has been challenging, and it became a reality with the generous help and encouragement of many people. I would like to extend my sincere appreciation to all of them.

First and foremost, I owe a deep sense of gratitude to my Ph.D. supervisor Dr. Kenji Nakahara for his guidance, continuous support and enormous help throughout my study. I would also like to acknowledge Dr. Jean-Luc Gallois and Dr. Kyoka Kuroiwa of the INRAE, GAFL, Montfavet, France, as well as Dr. Shamim Akhter of the Bangladesh Agricultural Research Institute (BARI), Bangladesh, for their valuable guidance. I extend my sincere gratitude to Prof. Dr. Shin-Ichiro Asano, Associate Prof. Dr. Masanao Sato from the Laboratory of Applied Molecular Entomology, and Prof. Dr. Hideyuki Matsuura from the Laboratory of Natural Product Chemistry, for their valuable feedback and critical review of this thesis. I am also thankful to Mrs. Miyuki Suto and Mrs. Kami Murakami, research associates, and all the members of the Laboratory of Pathogen-Plant Interactions for their help and support during my research experiments.

I gratefully acknowledge the Ministry of Education, Culture, Sports, Science and Technology (MEXT), of Japan, for providing the scholarship and opportunity to pursue my doctoral degree. I am also grateful to my friends for their love and support during my stay in Sapporo.

Finally, I express my deepest gratitude to my family and the Almighty Lord Krishna for their blessing and continuous encouragement throughout my years of study and research. This accomplishment would not have been possible without them. Thank you all!